KTH Industrial Engineering
and Management

Dynamic characterization of the tool holder material

An Experimental Thesis

Mayank Kumar

Master's Thesis

KTH Royal Institute of Technology

Department of Production Engineering

Stockholm

In collaboration with SSAB EMEA, Oxelösund, Sweden

Abstract

The major factors putting limitation to high productivity and good product surface quality is machining vibration. A lot of scientific research has been concentrated controlling the vibration while machining. There is a good sum of research going in department of production engineering at KTH to find out ways to reduce the machining vibration and enhancing the productivity but so far, they have been concentrated only on use of conventional steel as there of cutting tool. This they have tried by introducing damping in the conventional steel tooling system or by coating the tool with different composition of materials to improve the tool resistances to vibration.

In this paper, the research has been concentrated to finding out an alternative material to conventional steel, which is more resistance to machining vibration. The theory in the paper is mainly concentrated to give the basic understanding about frequency response function, forced vibration, and stability lobe diagram (SLD) and their applications. Through experimental modal analysis (EMA), machining tests and surface roughness of the machined surface (toolox 33 plates), SSAB toolox 44 steel cutting tool is compared against its counterpart the conventional steel (H13). The natural frequencies and damping factor are obtained for both free hanging and attached to machine condition. Afterwards, a stability lobe diagram is being plotted using the EMA data. Machining tests are being conducted according to SLD to their limits to determine and verify the material capability until tools starts showing vibrations.

In the end, the results is being compared by analyzing the sound emitted during the machining process and determining the surface roughness of the machined surface both visually and by white light interferometry. Then comparing the toolox 44 with conventional steel (H13), to find out which one is more resistance to vibrations.

Keywords: SSAB Toolox 44,SSAB Toolox 33, BOHLER-UDDEHOLM H13, Modal Analysis, Forced vibrations, Surface roughness, Machining, Frequency response functions.

Acknowledgements

This thesis work would not have been possible with the help and direction of certain people. It is my pleasure to thank two of my supervisors at the university Dr Lorenzo Daghini, Dr Andreas Archenti for their constant support, encouragement, and guidance. Dr. Per Hansson of SSAB EMEA AB support, guidance and providing materials for the experiments.

I would also like to thanks Tomas Österlind and Anton Kviberg for their help in setting up and running the experiments, and finally to my parents for their constant love and support.

The table of contents

Nomenclature and abbreviations_____ 8

1.Introduction

1.1Background_____ 9

1.2 Aim_____ 9

1.3 Brief introduction about experimental methodology_____ 10

1.4 Limitation_____ 10

2.Theory

2.1 Frequency response function_____ 11-12

2.2 Vibration in the machine structure_____ 12-14

2.2.1 Forced vibration_____ 14-15

2.2.2 Stability lobe diagram_____ 15-18

3.Method

3.1 Cutting tool material review [SSAB Toolox 44 & 33/ Bohler-Uddeholm H13]_____ 19-21

3.2 EMAs in cutting tool in free hanging condition_____ 22-24

3.3 EMAs in cutting tool loaded in machine condition_____ 24-25

3.4 Formation of SLD for finding out the machining_____ 25-26

3.5 Machining Test with different materials_____ 26-27

3.6 Surface measurement of the machined surface_____ 27-28

4.Results

4.1 Comparison between the compliance graphs for synthesized FRFs of two different cutting tool in free hanging condition_____ 29-30

4.2 Comparison between the compliance graphs for synthesized FRFs of two different cutting tool attached to the machine_____ 30

4.3 Stability lobe diagram of the cutting tool_____ 31

4.4 Machining of Toolox 33 plate at different Ap (mm) with toolox 44 and H13 cutting tool_____ 31

4.5 Analyzing recorded sound through microphone at different RPM and Ap_____ 32

4.6 Analyzing the vibration through waterfall diagram different RPM and Ap_____ 33

4.7 Surface measurement data_____ 33-34

4.8 Picture of machined surface_____ 34

5.Discussion and Conclusion_____ 35-36

6.Future work_____ 37

7.References_____ 38

Appendix I_____ 39

Appendix II_____ 40

Appendix III_____ 41-44

Appendix IV_____ 45-50

Appendix V_____ 51-52

Appendix VI_____ 53-54

List of Figure

Figure 2.1: The graphs represent (right) the dynamic compliance with different weight (left) the dynamic compliance with different stiffness

Figure 2.2: Various types of relative oscillations between tool and workpiece (a) axial oscillation (b) tangential oscillation (c) radial oscillation (d) tangential rotation

Figure 2.3: Closed loop system representing machining process

Figure 2.4: Stability lobe diagram (SLD)

Figure 2.5: Radial coordinates of the harmonic response locus

Figure 2.6: (Left side) Machined surface with chatter ;(Right side) machined surface without chatter

Figure3.1: (left) Toolox 33 plates (Workpiece/Dimension: 20x300x300 mm); (Right) Toolox 44 cutting tool

Figure 3.2: Graph showing dimensional change in H 13 steel after hardening and tempering

Figure 3.3: Cutting tool made of Bohler-Uddeholm H13

Figure 3.4: The distance between the sensors and their positon in different run in free hanging condition

Figure 3.5: The experimental set up of free hanging test. The sensors are attached to it with the help of wax and the whole set up is connected to the LMS test lab unit

Figure 3.6: The distance between the sensors and their positon in different run in loaded in machine condition

Figure 3.7: (Left) The experimental set up for the cutting tool (BOHLER-UDDEHOLM H13) is being shown and where the sensor (s1) and sensor (s2) (EMA Run1). (Right) The picture showing the workspace of 5-axis CNC machine (Hermle) is shown

Figure 3.8: Each slot is machined at different RPM and Depth of cut(Ap)

Figure 3.9: Insert used: ISCAR HM90 APKT 1003PDR IC 950

Figure 4.1: Synthesized FRF, compliance and phase for the cutting tool is X direction (Toolox-4331 Hz/ H 13 – 4334 Hz) [Toolox 44- Green; H13-Red]

Figure 4.2: Synthesized FRF, compliance and phase for the cutting tool is X direction (Toolox-1187 Hz/ H 13 – 1212 Hz) [Toolox 44- Green; H13-Red]

Figure 4.3: SLD of the cutting tools [Toolox 44- Green; H13-Red]

Figure 4.4: Graph showing at different different depth of cut Ap (mm) and RPM the tool made form toolox 44 and H13 is stable or not

Figure 4.5: Comparison of Throughput at 2000 rpm (left) Ap-0.50 mm [Toolox 44- Green; H13-Red]

Figure 4.6: Comparison of waterfall plot at 2000-rpm Ap-0.50 mm [Toolox 44- Green; H13-Red]

Figure 4.7: Comparison of Surface roughness (Left) H13 Ap-0.5mm Rpm-2000 (Right) Toolox 44 Ap-0.5mm Rpm-2000

Figure 4.8: Picture comparing the (Left) H13 Ap-0.5mm Rpm-2000 (Right) Toolox 44 Ap-0.5mm Rpm-2000

Nomenclature and abbreviations

Abbreviations (in alphabetical order):

DOF	Degree of Freedom
EMA	Experimental Modal Analysis
ESR	Electro Slag Re-melting
FRF	Frequency Response Function
MS	Machine structure
PV	Peak to valley
RMS	Root mean square
RPM	Rotation per minute
SLD	Stability lobe diagram

Nomenclature:

R_a	Surface roughness
K	Stiffness
ω_n	Natural frequency
Z	Damping ratio
M	Mass
P	Cutting force
d_c	Depth of cut
K_1	Coefficient of chip thickness
P	Cutting force
λ_s	Static stiffness

1. Introduction

1.1 Background:

Machining operation has become quite advance in recent decades. The significant changes which occur in the machining technology are the incorporation of numerical controlled machining. Understanding the metal cutting operation to increase the level of production has become a key topic but the topic has its complexities of itself due to the chip formation mechanism.

A problem still to be tackled is machining vibration which remains a subject of primary importance in modern manufacturing industry. To be able to remove high volumes of material in shorter time as well as to be able to get the right quality of the parts at the first time are goals that many shops would like to achieve. This will help them in producing more number of products in less time thus bringing down the cost of production and help them earn more profit. A recent cost study done by Renault group on their cylinder dead production line showed that yearly out of three million parts produced by them the money which they lose due to machining vibrations is 0.35 euros per cylinder[1]. The development of science, technology, and technique, and the pressure of competitive markets have driven the expansion of manufacturing frontiers. Despite of all these advances chatter vibration has been for the last sixty years is limiting the improvement in productivity and part quality in metal removal process. Thereby, It is the most popular topic for research in the academic and industrial research community[2].

In the thesis, the comparison is being made to find the alternative steel which performs better than the conventional steel in resisting towards machining vibrations.

1.2 Aim:

The aim of the thesis is to stablish if, using different materials for machining operation, in this case SSAB Toolox 44 improves the tool's resistance to vibration than the conventional steel. Hence, understanding the usage of Toolox 44 cutting tool and its future scope. More

specifically, the study is conducted on the dynamic properties of material and its usage as cutting tool. It is limited to analyse the nature of different materials in milling operations.

1.3 Brief introduction about experimental methodology:

1. The comparison of SSAB Toolox 44 and BOHLER-UDDEHOLM H13 steel in the form of cutting tools is conducted via Experimental modal analysis (EMA) in condition such as free hanging and attached to machine. EMA gives the dynamic behaviour of the cutting tool such as natural frequency, static and dynamic stiffness, phase, and damping ratio are derived by the compliance graph.

2. The stability lobe diagram (SLD) is being created from the results obtained from EMA attached to machine condition. The SLD shows the behavioural trend of the cutting tool resistance towards vibrations.

3. Both the tools underwent metal cutting test (milling) on toolox 33 plates using the same cutting parameters. The cutting parameters are based on the behavioural trends shown in the SLD. The responses such as surface roughness, vibration, and acoustics are being compared in the end to get the results.

1.4 Limitation:

The budget and time issue where the major limiting factors. Thereby, the cutting tool is being compared with toolox 44 steel and H13 steel, not with the cutting tool or on the workpiece made up of different steels or tool made of different configurations. The testing conditions such as cutting parameters or different L: D ratio are being kept very restricted and in a small envelope. Otherwise, it would be very difficult to make comparison between the data obtained from EMA and machining operation as it contains lot of variations.

2. Theory

2.1 Frequency response function:

In the chapter, the basic of vibration analysis for the linear structure with single degree of freedom is being explained in details. The physical characteristics of the any structure are usually determined by mass, stiffness and damping ratio, which are referred as Spatial Modal. To determine the behavior of any structure, an analytical modal analysis is conducted to finding out natural frequencies, vibration mode shapes, and modal damping factors. The convenient way to represent the structural response is through response modal which a set of FRF. There are six different types of FRFs such as Dynamic compliance, Mobility, Inertance/ Accelerance, Dynamic stiffness, Mechanical Impedance, Apparent mass. While plotting the FRFs the factors that can affect the output are Noise, Spectral leakage, Non-linear distortion[3].

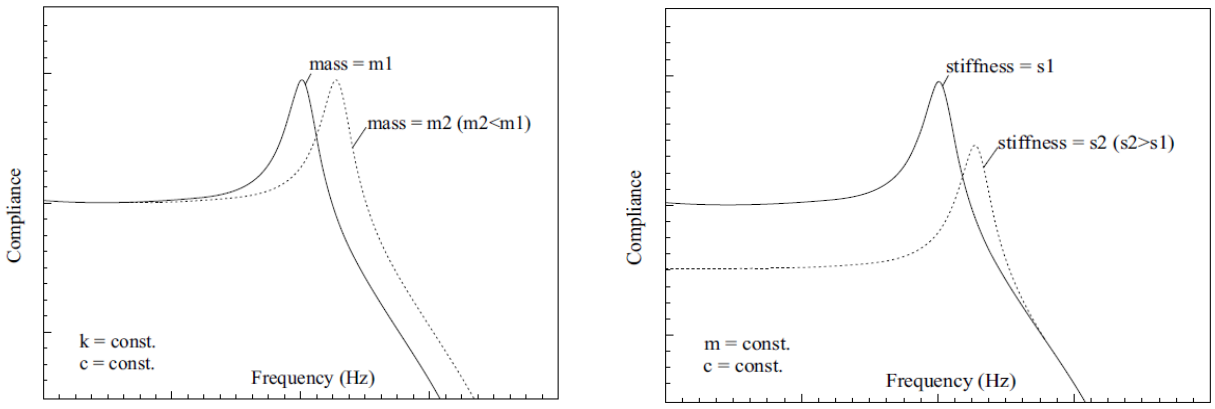

Figure 2.1: The graphs represent (right) the dynamic compliance with different weight (left) the dynamic compliance with different stiffness[4].

The figure 2.1 shows one out of six different FRFs, which is dynamic compliance graph. The advantage of having a compliance graph as a result is that, it gives all the modal data such as amplitude, phase, stiffness, natural frequency, and damping ratio, which is, need to know of

the material. Not these all parameters are available in the Inertance plot as they only show the phase, natural frequency and damping ratio of the structure. The output given by the accelerometer is Inertance plot. The compliance plot of different weight materials is shown in figure 2.1(left) that the natural frequency of the both the material is different, as it depends upon the mass of the tool.

$$\omega_n = \frac{1}{2\pi}^2 \sqrt{\frac{k}{m}} \quad (2.1)$$

From the equation 2.1, it is being deduced that the structure with lower mass should have a higher natural frequency than the object with higher mass. Thereby, the stiffness will have higher of the object with higher mass. From the figure 2.1 (right), the object with higher stiffness will have a reduction in amplitude, as both of them are directly proportional to each other. The tools with higher dynamic and static stiffness are more accuracy and productivity while machining as the deflection is less from those tools with lower stiffness. Lower deflection while machining means that the cutting tool is less prone to forced and self-excited vibration[3].

2.2 Vibration in the machine structure:

Traditionally, the machining is being considered, as a steady state process i.e. the cutting process will have a constant feed, speed, cutting angles and chip thickness. To achieve a stable cutting operation the resultant force is to remain constant, which is not possible in a real life scenario. The cutting force around an average value leads to relative deflection between the tools and the workpieces. This defection produces a variation in the speed, cutting angles and chip thickness. Thereby, steady-state processes are not possible in reality. The non-steady state in the metal cutting process becomes more visible under the chatter condition. Hence, the chatter theory is to undergo through the dynamic metal cutting and understanding when and how the chatter happens. It is hard to study the dynamics of metal cutting in isolation. So special experiments are designed in which the parameters are varied in a controlled manner to investigate the oscillation of tools[2].

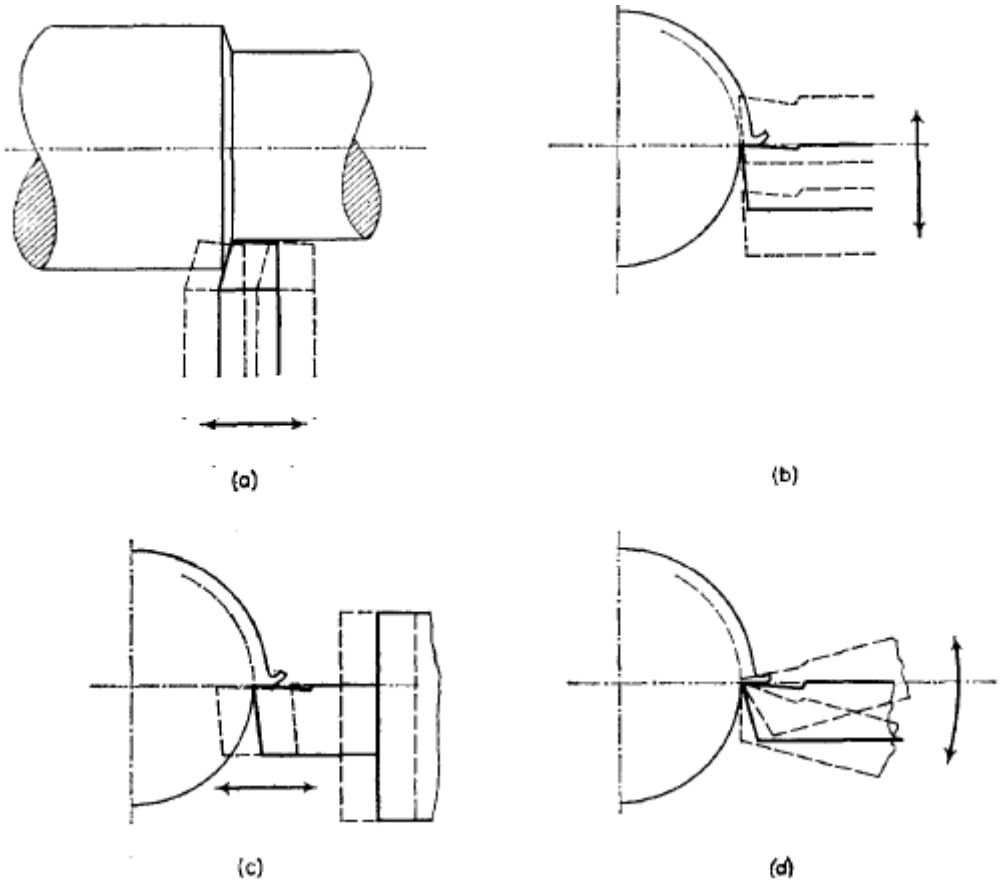

Figure 2.2: Various types of relative oscillations between tool and workpiece (a) axial oscillation (b) tangential oscillation (c) radial oscillation (d)tangential rotation[5].

Chatter in the machining system leads to limitation in the productivity of the machine and many other disadvantages like rough surface of the machined part, tool chipping, and unwanted noise on the production floor. Kδ factor, introduced by Tobias which stated that the cutting process is dependent the factor like damping and stiffness. To achieve improvement in the process a trade-off has to be done between these two factors. There are two types of vibrations such as forced and self-generative vibration [5, 6]. In the figure 2.3, the line diagram of a closed loop system representing the dynamics of machining can see seen.

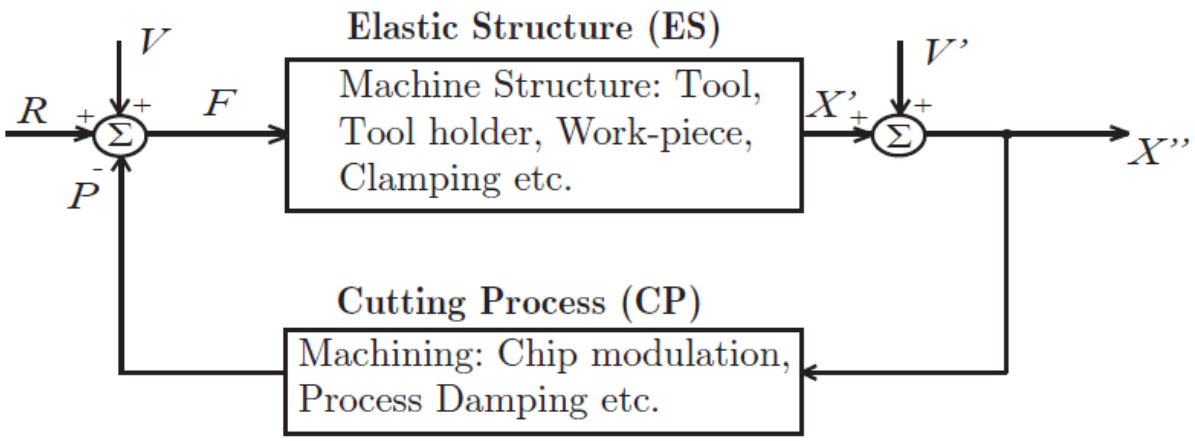

Figure 2.3: Closed loop system representing machining process[7].

In the figure 2.3, R represents the reference signal which shows the position of the tool relative to the workpieces. V represents the outer disturbance in the system such as scale error. The displacements of tool on the workpieces can be notice from its reference point when R & V are combined together gives another position called X'. On the output side of the system V' which is the second outer disturbance combines with X' give the true position of the tool which is X''. As the system turns out to be a close looped system the shift in the position, leads to a feedback signal which leads to change in the cutting force P[7].

2.2.1 Forced vibration:

The forced vibration occurs due to repeated entry and exit of cutting teeth in the machining process leads to forced vibration. This leads to development of a fluctuating force from the motion by the workpiece or tool. It can happen due to external and internal time varying forces, which leads to generation of an intermittent cutting force. The magnitude of the force is highly dependent on the impact of teeth on the entrance whereas the released of potential energy is being determined by the angle at which the teeth's exists. The impulse generated by the impact, which then excites the machine structure (MS) in a broad band.

High vibration and surface distortion can be achieved if the forced vibration is closer to the eigen frequency of the MS. To find out whether there is a forced vibration during the process. The sound emitted is recorded during the machining process at different cutting speed. At all cutting speed if it shows the same frequency peak, as it shows at the structural resonance then, the process is subjected to forced vibration. Increasing the number of teethes in the cutting tool will minimized or stops the forced vibration and increase the

damping coefficient. An increase in number of teeth leads to smaller impact force and potential energy build up which tends to reduce the amplitude of vibration. Damping also plays an important role in minimizing the forced vibration, so the enhanced damping measure can also be included to stop it[7].

2.2.2 Stability lobe diagram:

The stability lobe diagram (SLD) is being plotted to tackle chatter occurrence of in machining operation. The graphical form takes into account the rotational speed of the tool or workpiece even where the structure of the machine is not well define. From the figure 2.4, the region under the graph is the stable region. The stable regions extends until a certain rpm depending upon the material which is undergoing cutting and the material of which cutting tool is made off. The unstable region is the area above the graph were regenerative chatter occurs.

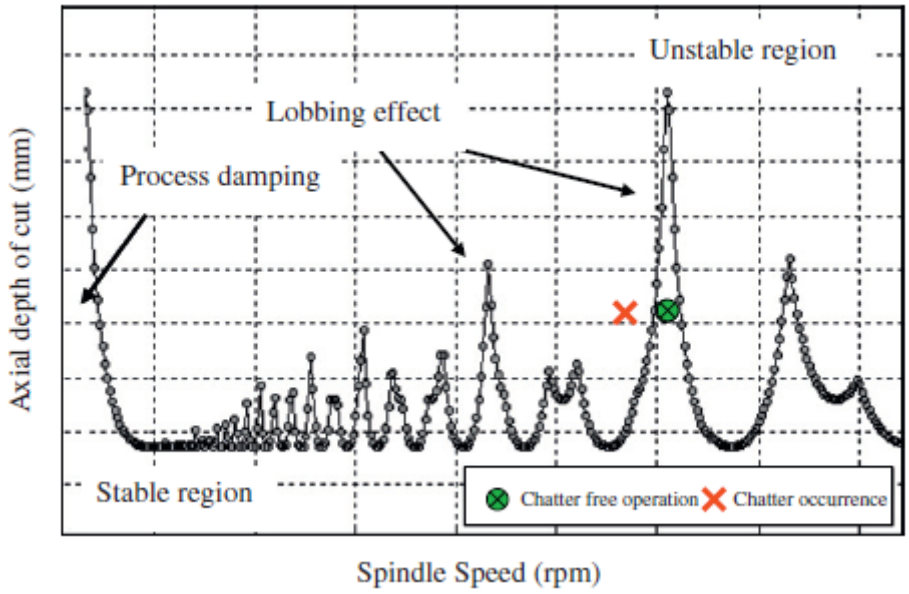

Figure 2.4: Stability lobe diagram (SLD) [2].

The regenerative chatter is a self-excited oscillation, which occurs in the system. In the cutting process, if any disturbance is observe a relative vibration is being induce in the process that leads the tool to start defecting form its predefined path. Therefore, the stability chart is being prepared for forecasting the dynamic behavior of the structure. SLD is prepared considering the motion between tool and workpiece normal to the cutting surface. If the motion of the tool is not controlled, the waviness on the surface of the workpiece will

appear. Hence, there is degradation in the surface quality of the workpiece which in turn effecting the dimensional accuracy of it[8].

Now, the discussion would be about the how to derive SLD mathematical. The cutting force P is the function of width, depth of cut and cutting speed. To change the cutting force (P) alteration in the cutting speed is required while keeping the depth of cut unaltered. Hence, the equation form is:

$dP = k_1 [x(t)-x(t-T)]$ (2.2)

Where k_1 if the coefficient of the chip thickness, T is the time of rotation. The force vibration applied by machine is in the same direction as the cutting force gives the harmonic force $F\cos \omega t$. Hence, the equation is:

$F(\ddot{x},\dot{x},x) = F\cos \omega t$ (2.3)

The equation 2.3 is widely known as equation of the motion where x, is the relative displacement of the surface. $F(\ddot{x},\dot{x},x)$ is the function of the tool at the frequency range when the machine structure is excited. In figure 2.5, a harmonic response locus in radial coordinate system is being plotted taking into account ω as a functional displacement of x w.r.t. time.

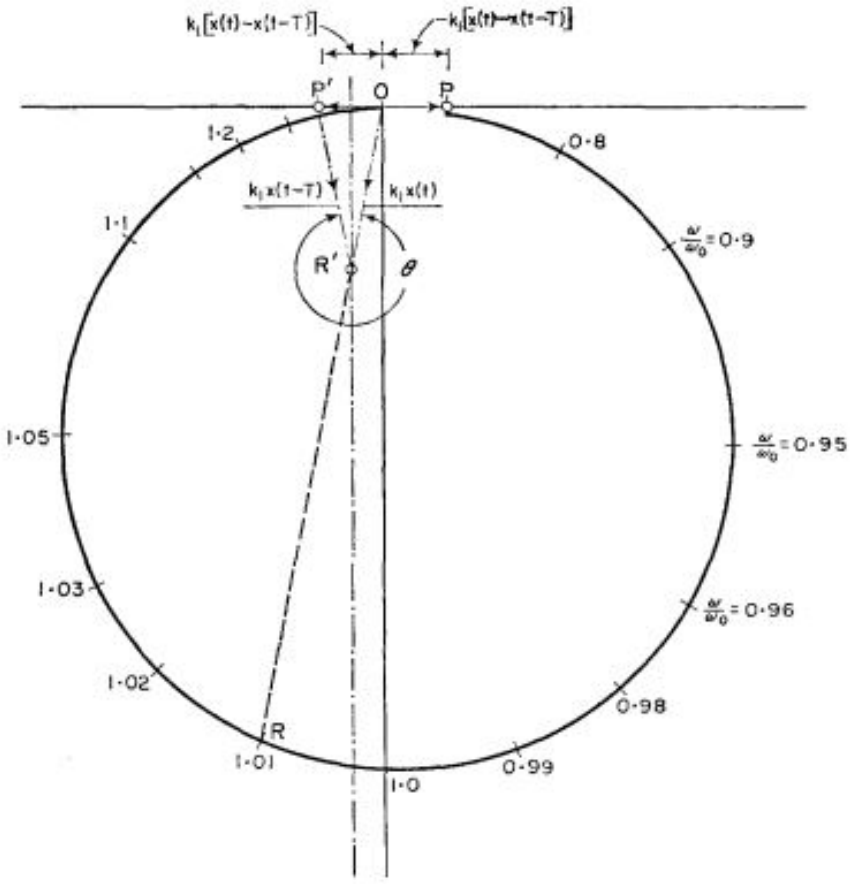

Figure 2.5: Radial coordinates of the harmonic response locus [6].

Static stiffnessλs is multiplied to find out the normalized radial coordinate leading to force calculation. In the figure, OP shows the direction where the force is going to act give the static displacement equation x_s = F /λs. As the equation for the steady state needed, Fcos ωt is interchange with the incremental force dP (t). Hence, the equation obtained is:

F ($\ddot{x}$,$\dot{x}$, x) = - dP (t) (2.4)

The negative sign in equation 2.4 is because the opposing force comes into effect while putting the cutting force on the workpiece.

F ($\ddot{x}$,$\dot{x}$, x) = - k_1 [x (t)-x (t-T)] (2.5)

Since x (t) at its stability limit is sinusoidal which gives the direction of the cutting force OP^1 vector (OP^1=OP). OP^1 vector has two other vectors k_1x (t) and k_1x (t-T). From the figure 2.5, it can be deduced that these two vectors OR^1= k_1x (t) and P^1R^1= k_1x (t-T) are the perpendicular

bisector of the force vector OP^1 which allow to complete the triangle. Both the vectors are of equal magnitude. After putting the normalization in the equation, it turns out to be:

$$\frac{k_1}{\lambda s} = \frac{OR^1}{OR} \qquad (2.6)$$

Equation 2.6, gives the chip thickness coefficient for the chatter, which occur at the frequency given by R from the figure 2.5. Hence, the stability chart is being plotted taking k_1 as a function of the rotational speed for the stable and unstable condition [6, 9].

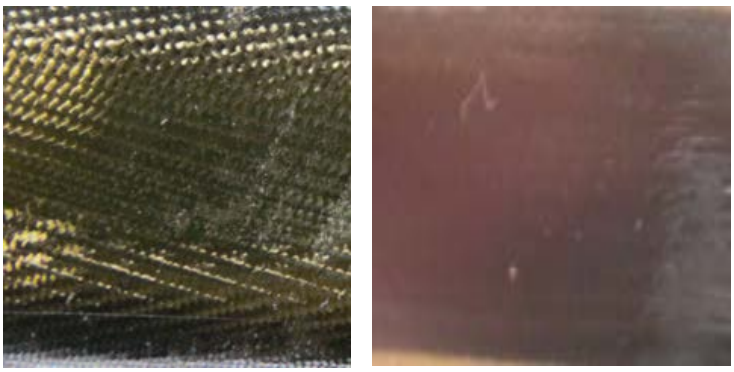

Figure 2.6: (Left side) Machined surface with chatter ;(Right side) machined surface without chatter.

3. Experimental Methodology and discussion

In this chapter, there are discussions about the materials, cutting tool specification, EMA, SLD, machining operation and the methodology by which the experiments were conducted and in which order.

3.1 Cutting tool material review [SSAB Toolox 44 & 33/ Bohler-Uddeholm H13]:

"**T**oolox is a modern quenched and tempered pre-hardened tool and machine steel delivered with measured and guaranteed mechanical properties."[10] Toolox has low carbon content similar other steel but specially developed for tooling and machining operation.

The two different types of Toolox that has been used: Toolox 33(workpiece), which has a hardness of 300 HBW and Toolox 44(cutting tool), with a nominal hardness of 45 HRC. It is a pre-harden steel with same level of hardness all the way through. Toolox are pre-heated and ready to use steel. It lowers the cost and time of production due to its high machinability. These properties make toolox a versatile steel that can be used in a wide spectrum of activities. The chemical composition, physical and mechanical properties of the Toolox 33 & 44 can be find in appendix 1.

Toolox is two to three times' higher toughness when compared to any other steel of similar hardness, which is due to high cooling rate and low carbon presence. The steel has high toughness and hardness that makes it more resistant to surface wear. The material is capable of working in high temperature environment while keeping its high strength and toughness. These all properties comes in toolox due to change in the carbide morphology, which has been due to high cooling rate during quenching operation and due less carbon content. Toolox comes with Electro Slag Re-melting (ESR) properties. One of the main advantages using toolox is that, it has a very low residual stress than other steel in his class due to the high tempering temperature. This leads to avoid stress relieving process even after many hours of heavy machining. The high level of machinability is due to the low carbide content[10].

Figure3.1: (left) Toolox 33 plates (Workpiece/Dimension: 20x300x300 mm); (Right) Toolox 44 cutting tool.

Cutting tool specification and characterization:

Manufacturer:	ISACR	Length (L):	150 mm
Material used:	Toolox 44	Inserts (Z):	3
Weights:	340 gm		
Type of inserts used:	ISCAR HM90 APKT 1003PDR IC 950		

Bohler-Uddeholm H13 steel is a conventionally produced hot work tool steel with overall good ductility, toughness, wear resistance, hardenability, and machinability. To provide an overall product consistency and uniformity the H13 steel is specially processed .H13 is a chromium-molybdenum-vanadium alloyed steel. It shows a good resistance towards abrasion both at high and low temperatures. The steel shows remarkably high level of toughness, ductility, machinability, and polishability .H13 steel is also quite resistance to thermal fatigue and shows high strength at a high temperature.

The H13 steel has to go through heat treatment process which might be annealing, stress relieving or hardness process like quenching, tempering after a rough machining on it. To again regain its lost physical properties lost during the process. Quenching process is used to obtain certain mechanical properties like hardness. The material has to go through tempering process to increase the toughness of the steel. As the quenching operation make the steel excess harder hence making it brittle. To remove the excess hardness the exact tempering temperature is determined according to the chemical composition of the H13 and

type of desire properties expected from it[11]. The chemical composition, physical and mechanical properties of the H13 can be find in appendix II.

In the figure 3.2, the dimension change can be seen in H13 steel when it goes through hardening and tempering process.

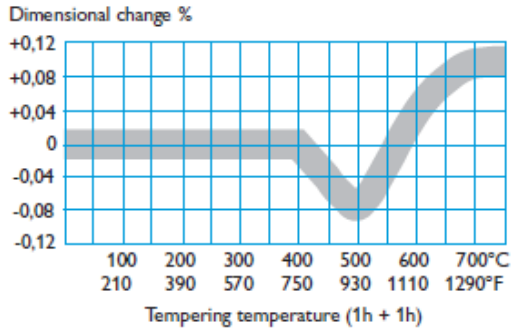

Figure 3.2: Graph showing dimensional change in H 13 steel after hardening and tempering[11].

Figure 3.3: Cutting tool made of Bohler-Uddeholm H13.

Cutting tool specification and characterization:

Manufacturer:	ISACR	Length (L):	150 mm
Material used:	Bohler-Uddeholm H13	Inserts (Z):	3
Weights:	291 gm		
Type of inserts used:	ISCAR HM90 APKT 1003PDR IC 950		

3.2 EMAs in cutting tool in free hanging condition:

Experimental modal analysis by impact testing is a useful and simple tool in obtaining the set of modal parameters. These set of modal parameters are used to find the dynamic property of the holders[3].

In the free hanging test, the cutting tool hangs with the help of an elastic string as long as possible to simulate a free hanging condition for the modal analysis. A nut is being gulled on the top face of tool, which is then used to hang the holder. This procedure is applicable for the all the different cutting tool. The sensor points are marked at three different point aligned to each other at a known distance as shown in figure 3.4. The points that are marked on the tool are just for the reference basic to keep the similarities of test between two individual. These markings on the tool help in standardizing the experiments.

The EMA is being conducted on the cutting tool in two steps by just changing the position of the sensors form point 1 to point 3 and keeping the point of impact on point 2. The method is known as fixed hammer method (where the accelerometer moves in between every measurement). All the double hits by the hammer are rejected and the result is the average of five individual hits. Two sets of EMAs are performed on the workpiece.

Note: The impact is on the opposite side of sensor two to obtain sinusoidal wave.

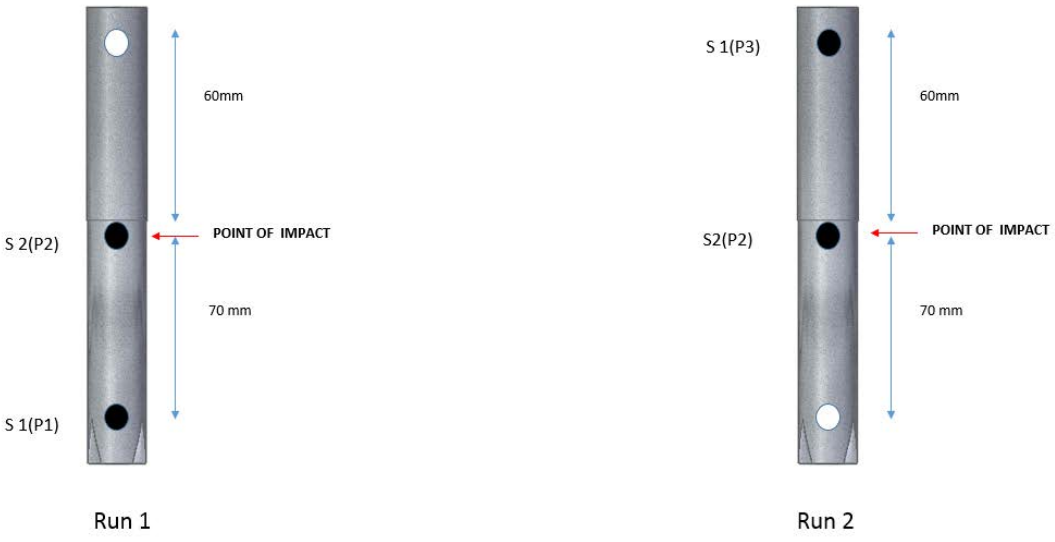

Figure 3.4: The distance between the sensors and their positon at different run in free hanging condition.

Figure 3.5: The experimental set up of free hanging test. The sensors are attached to the cutting tool with the help of wax and the setup is connected to the LMS test lab unit.

Specification of accelerometer :

Sensor 1:			
Brand:	Dytran	Model:	3225F
SN:	6284	Sensitivity:	10.3 mV/g
Weight:	0.6 gm		
Sensor 2:			
Brand:	Dytran	Model:	3225F
SN:	6284	Sensitivity:	9.6 mV/g
Weight:	0.6 gm		

Specification of the hammer:

Brand:	Ziegler	Model:	Ixys H2
SN:	9117	Sensitivity:	2.24mV/N
Attached weight:	77gm	Tip:	Steel

Data acquisition system: LMS test lab Rev 11 Impact testing on College computer.

3.3 EMAs in cutting attached to machine:

The second step is to run the EMAs on the cutting tool when it is being attached to machine structure. The machine used is an in-house Hermle a 5-axis CNC machine. All the cutting tools are inserted 5 cm inside the collet based tool holder, which holds the tool at one point. The tightening of the cutting tool is done in the same way for all the different tools. The L: D ratio is the kept the same, i.e. the tool over hang is the same for the EMA. The three sensors points that are marked on the holder are just for the reference basic to keep the similarities of test between two individual and to standardizing the experiments.

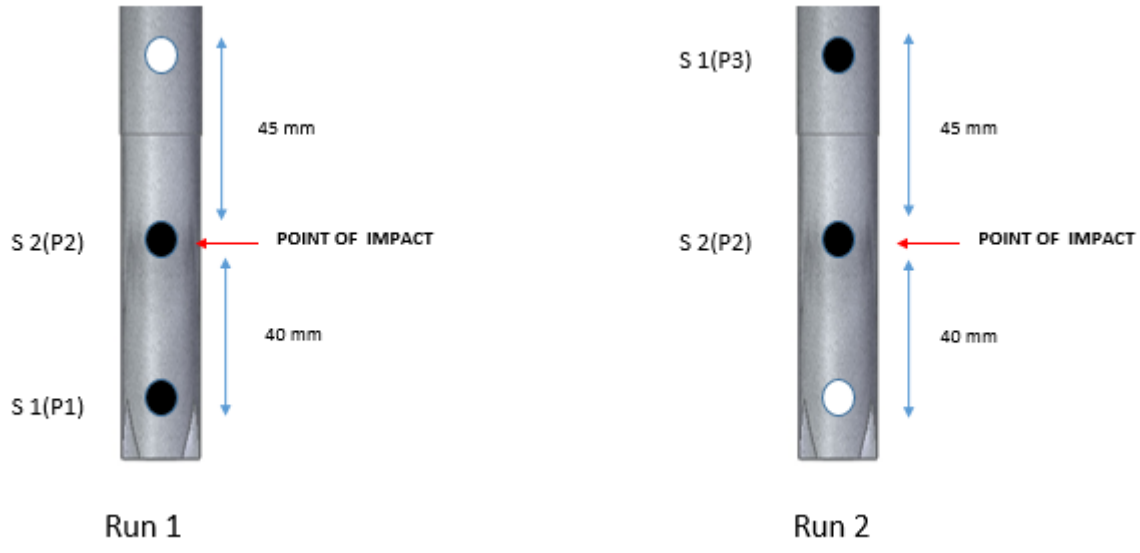

Figure 3.6: The distance between the sensors and their position in different run in loaded in machine condition.

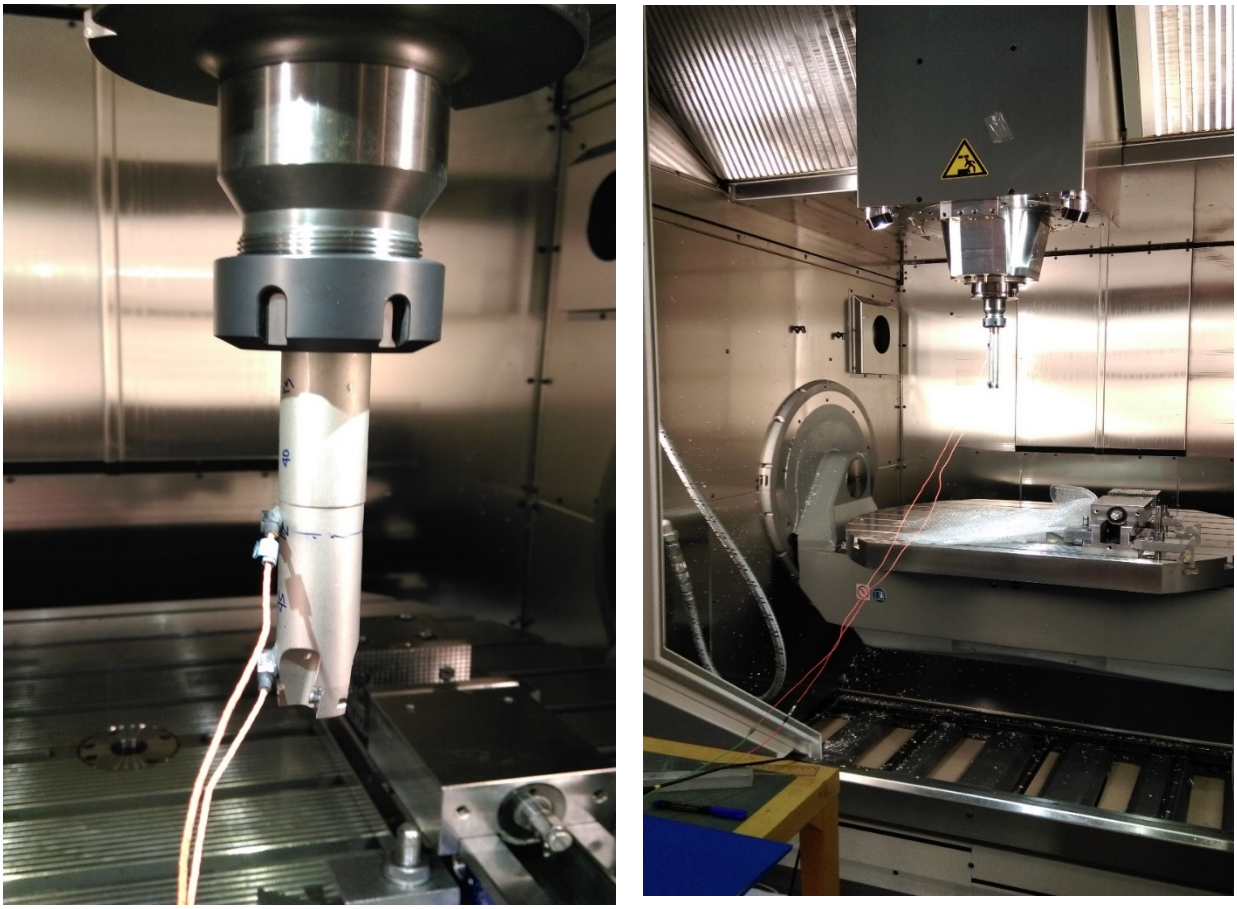

Figure 3.7: (Left) The experimental set up for the cutting tool (BOHLER-UDDEHOLM H13) is being shown and where the sensor (s1) and sensor (s2) (EMA Run1). (Right) In picture, the workspace of 5-axis CNC machine is shown.

Data acquisition system: - LMS test lab Rev 11 Impact testing on College computer.

3.4 Computation of Stability lobe diagram SLD:

The motive of plotting the SLD is to compare the tool materials and foresee the actual behavior during machining operation. The modal parameters data such as eigen frequencies, damping, stiffness are used when the cutting tool is attached to the machine (as it is more realistic than free hanging condition) are entered into a Matlab script[7]. The force coefficient for toolox 33 is not available that is why normal steel (2000 N/mm^2) is chosen since its cutting force coefficient lies much closer to the toolox 33. In this way, the graph is not accurate but close enough to run the machining test. The cutting tool has three tooth and in slotting operation, the cutting angle is 180°. The total teeth engaged during the

cutting operation are 1.5 teeth's is taken into account but process damping is not being considered while plotting the SLD.

3.5 Machining Test:

The cutting tests are designed keeping in mind the limitation of the inserts and the machine on which it is going to run. While designing the experiments the cutting speeds are chosen by referring to the SLD, performance range of the inserts and the diameter of the tool. The experiments are designed keeping the feed rate constant in all the sets of the experiments. The cutting operation is slot-milling operation that is done along the length of the workpiece. In the table below all the RPMs and Ap the test has run on can be seen.

RPM	2000	2200	2300	3000	4000
Ap (mm)	0.4; 0.45; 0.5; 0.55; 0.6	0.3; 0.4; 0.45; 0.5; 0.6; 0.65	0.3; 0.4; 0.5	0.1;0.2; 0.3; 0.4; 0.5; 0.6	0.1;0.2; 0.3; 0.4; 0.5

Figure 3.8: Each slot is machined at different RPM and depth of cut (Ap).

A microphone is installed inside the CNC machine perpendicular to the workpiece to record the sound and find out at which depth of cut, the system is acting stable or unstable. The sound recorded by the microphone contains both unwanted sound (such as sound of the coolant jet and sound of the workspace) and the wanted sound from the cutting process. The throughput and waterfall chart is being plotted in the real time.

Specification of the inserts:

Brand:	ISCAR	Model :	IC950
Cutting speed (V_c) :	80-350 m/min	Weight:	1.824 gm
Feed rate(F_z):	0.08-0.15 mm/t	Depth of cut (A_p):	4mm-8 mm (Normal steel)

Specification of the CNC machine:

Brand:	Heidenhain TNC 640	Model:	C 50UMT
Operation Type:	CNC	Num. of Axes:	5
Work support:	Table	Top RPM:	1200
Column:	Multi/Bridge	Column Style:	Travelling

Specification of the microphone:

Brand:	PCB Piezotronics	Model:	378B02
SN:	116691	Sensitivity:	50 mV/Pa

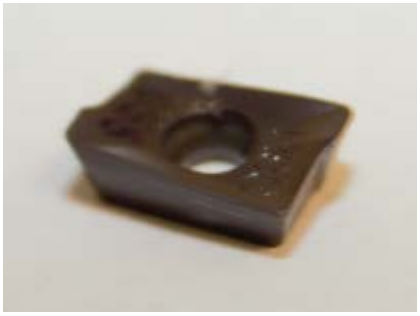

Figure 3.9: Insert used-ISCAR HM90 APKT 1003PDR IC 950.

Data acquisition system: - LMS test lab Rev 11 Signature acquisition on College computer.

3.6 Surface measurement of the machined surface:

Surface measurement process is one way to find out the more information about the material behavior. Replication process is used, as the plates are too big and heavy for any surface roughness measuring instruments workspace. The replicas are measured using the white light interferometry, Zygo New View^{TM} 7300 to find out the 3D surface roughness of the machined surface. The measurement area for the all samples is 1.09 x 1.09 mm^2. Peak to

valley (PV), RMS, R_a are being calculated over the entire sample sizes. The surface roughness R_a is calculated taking the average of five 0.8 mm traces all over there sample size.

Specification of Replica:

Brand:	Microset	Fluid :	101RF
Curing time:	5 mins	Working life:	30 sec@ 25°c

Specification of the White light interferometry:

Brand:	Zygo	Model:	Nv 7300
Description:	Optical profiler	Max Scan Range:	≤20 mm
Scan Speed:	≤135 µm/sec	Objectives:	From 1X to 100X

4.1 Comparison between the compliance graphs for synthesized FRFs of two different cutting tool in free hanging condition:

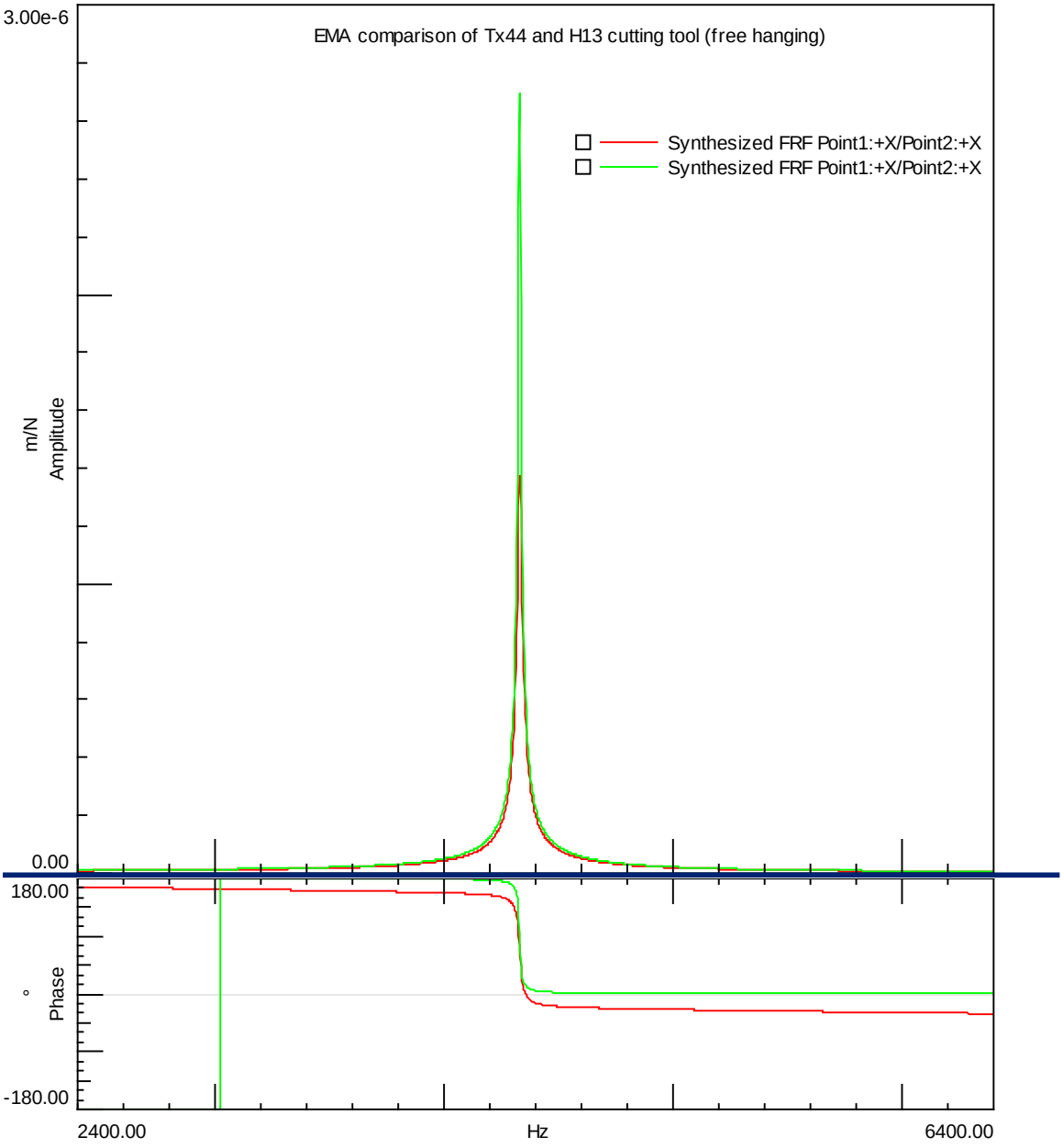

Figure 4.1: Synthesized FRF, compliance and phase for the cutting tool is X direction (Toolox-4331 Hz/ H 13 – 4334 Hz) [Toolox 44- Green; H13-Red]. From the compliance graph, it can be seen that both the cutting tools which are made of different materials, weight, but same specifications showed almost same natural frequency. As it can be seen from cutting tools specifications that, the tool made from toolox 44 is heavier. Hence, it should have shown

much less natural frequency than H13 cutting tool (Ref chapter 2). Thereby from equation 2.1, it can be concluded that toolox is stiffer and has a higher young's modulus than H13.

4.2 Comparison between the compliance graphs for synthesized FRFs of two different cutting tool attached to the machine:

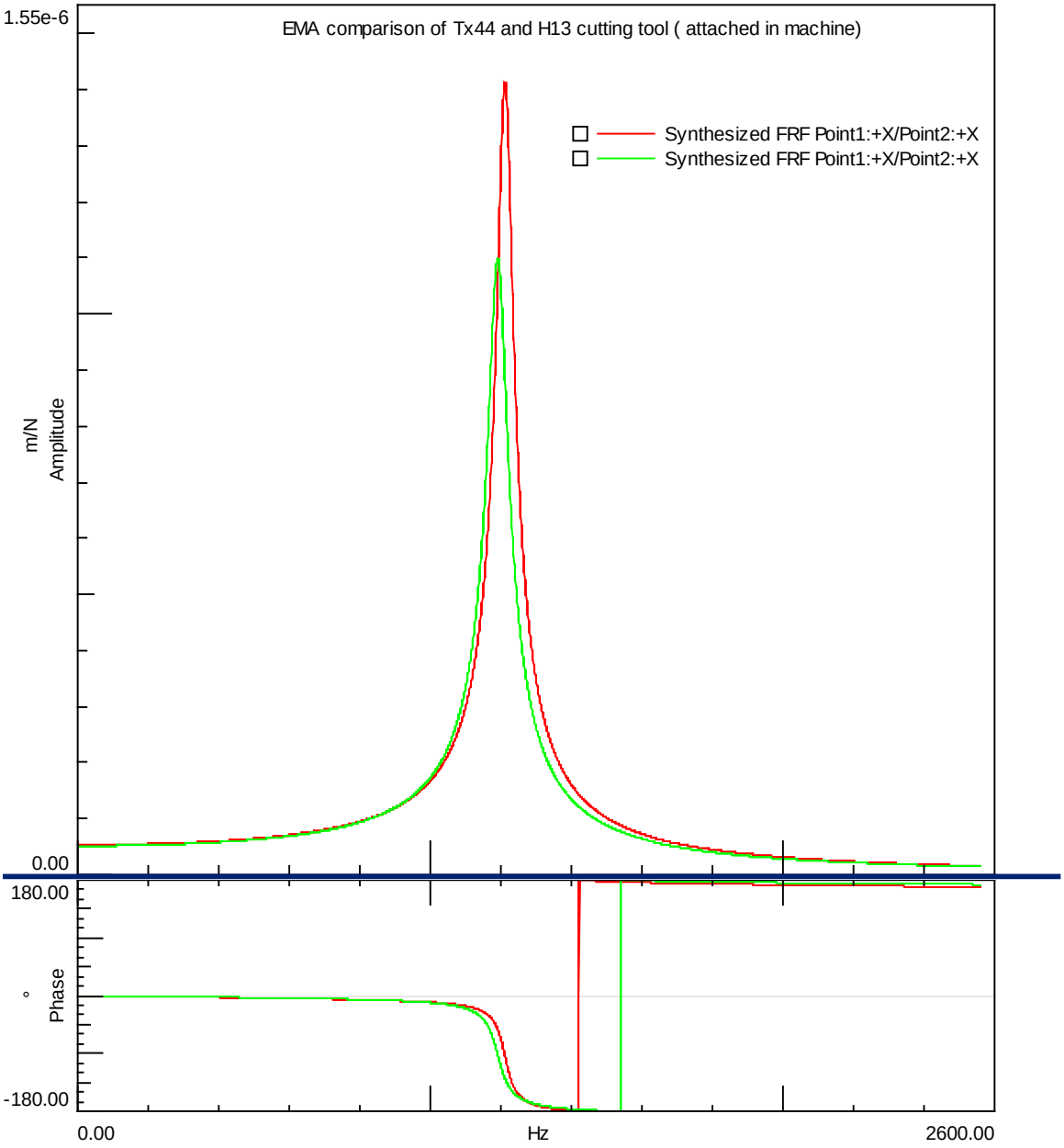

Figure 4.2: Synthesized FRF, compliance and phase for the cutting tool is X direction (Toolox-1187 Hz/ H 13 – 1212 Hz) [Toolox 44- Green; H13-Red]. After the free hanging test is conducted, the tool is being attached to the CNC machine and model analysis is being performed under similar condition (i.e. same L: D ratio/ tool overhang).The compliance graph plotted from the test showed that eigen frequency of the toolox 44 is less than H13 tool. Thereby, proofing our hypothesis that toolox 44 is much stiffer than H13.

4.3 Stability lobe diagram of the cutting tool:

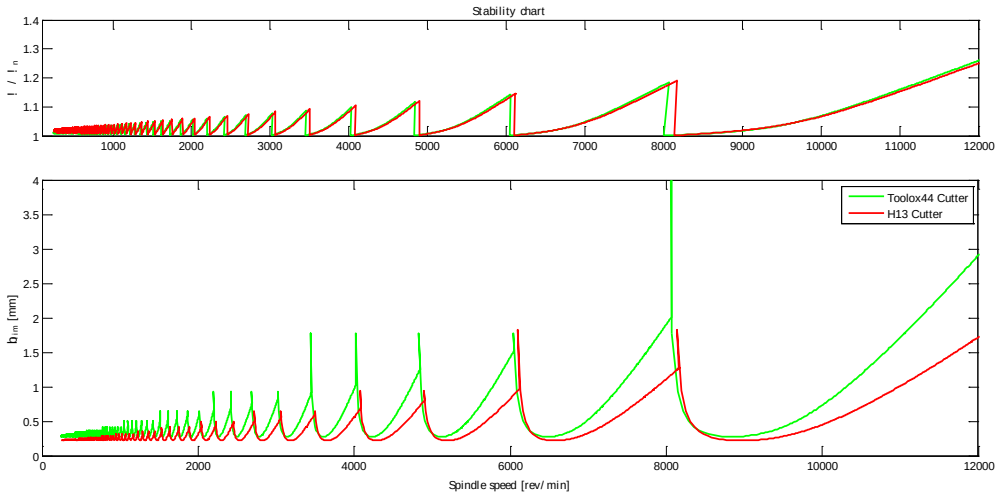

Figure 4.3: SLD of the cutting tools [Toolox 44- Green; H13-Red]. The SLD is being plotted with depth of cut on the X-axis (assumed for normal steel) and on the Y-axis is the spindle speed (the maximum RPM of 5-axis CNC/Hermle).From the SLD plot, it can be seen that toolox 44 cutter shows more resistance to vibration even at higher depth of cut than the conventional steel.

4.4 Machining of Toolox 33 plate at different Ap (mm) with Toolox 44 and H13 cutting tool:

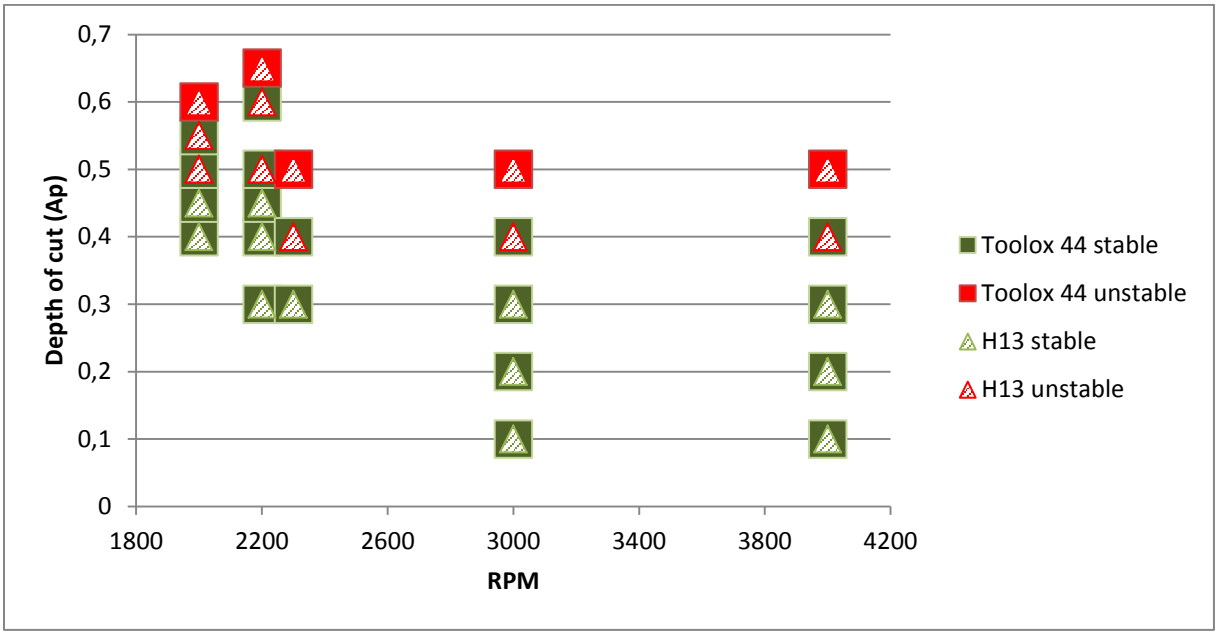

Figure 4.4: Graph showing at different depth of cut Ap (mm) and RPM, the tool made form toolox 44 and H13 is stable or not. From the graph, it can be seen that which all rpms and depth of cuts the machining operation has run-on and at which experiment set the system is stable and at which point it unstable both for toolox 33 and H13 steel.

4.5 Analyzing recorded sound through microphone at different RPM and Ap:

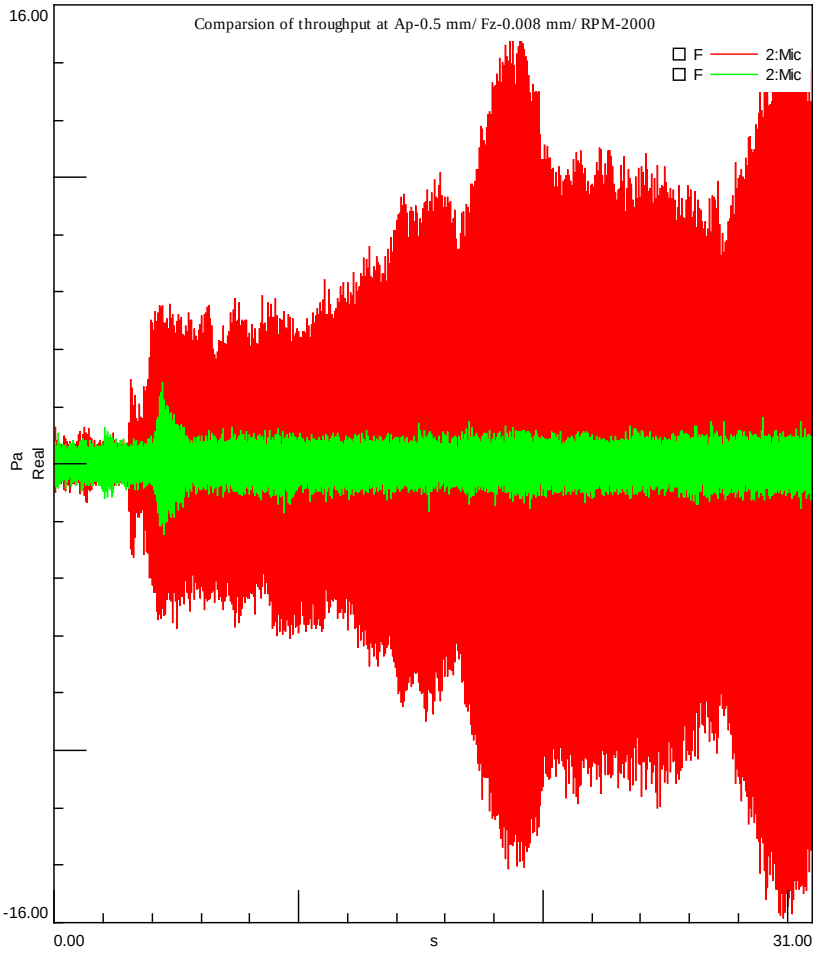

Figure 4.5: Comparison of Throughput at 2000 rpm (left) Ap-0.50 mm [Toolox 44- Green; H13-Red].The throughput plot is being plotted from the sound recorded by the microphone while machining. In this comparison at 2000 rpm, 0.50 mm depth of cut and constant feed rate H13 shows significant amount of chatter while Toolox 44 remains stable all the way till end of machining process.

(Ref to Appendix III for more throughput diagram at different RPM and depth of cut)

4.6 Analyzing the vibration through waterfall diagram different RPM and Ap:

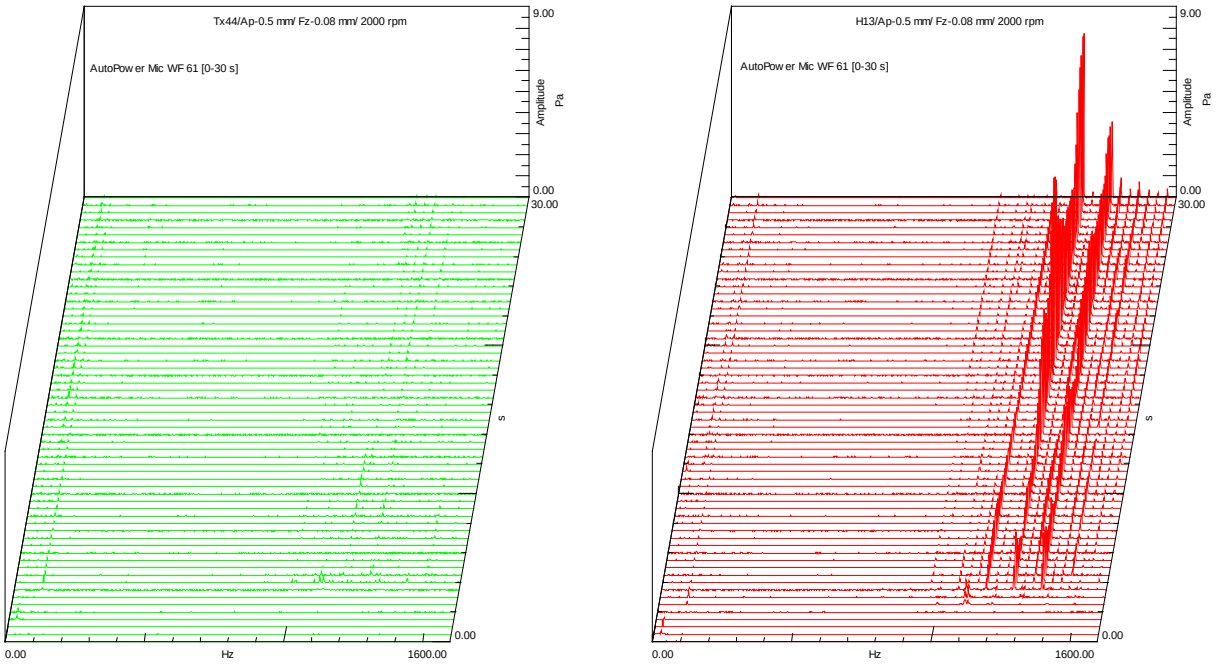

Figure 4.6: Comparison of waterfall plot at 2000-rpm Ap-0.50 mm [Toolox 44- Green; H13-Red].From the waterfall graph, it can be observed in H13 plot the gradually increase in the amplitude which leads to chatter build up in the system. The chatter build starts nearly at the same eigen frequency that has obtained by EMAs of the tools for the H13 when it is attached to the machine. Since, toolox 44 has a higher stiffness than H13; the amplitude did not reached the point where the chatter can be observed in the system.

(Ref to Appendix IV for more waterfall diagram at different RPM and depth of cut)

4.7 Surface measurement data:

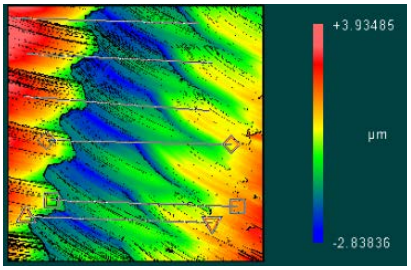

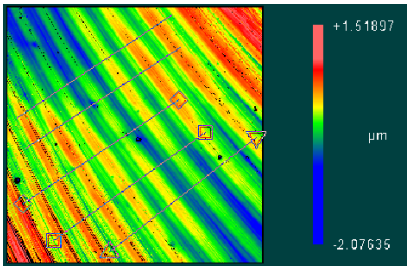

PV	6.773 µm	PV	3.595 µm
RMS	1.318 µm	RMS	0.357 µm
R_a	1.102 µm	R_a	0.287 µm

Figure 4.7: Comparison of Surface roughness (Left) H13 Ap-0.5mm Rpm-2000 (Right) Toolox 44 Ap-0.5mm Rpm-2000.The surface measurement values of the machined surface are obtained by a white light interferometry. The effects of chatter can be easily being seen on

the surface machined at this specific parameter by H13 cutting tool, which is showing higher R_a than surface machined by toolox 44 cutting tool.

(Ref to Appendix V for more surface measurement data at different RPM and depth of cut)

4.8 Picture of machined surface:

Figure 4.8: Picture comparing the (Left) H13 Ap-0.5mm Rpm-2000 (Right) Toolox 44 Ap-0.5mm Rpm-2000.The difference in the surface roughness on the surface is also visible by the naked eyes.

(Ref to Appendix VI for more pictures at different RPM and depth of cut)

5. Conclusion and discussion

The EMA of the cutting tool is being done in free hanging condition. From the compliance graph (ref. figure 4.1) the observation can be made that both the cutting tool has almost same natural frequency but toolox shows higher amplitude than H13 .From chapter 2, It is concluded that if the weight of tool is more, it will show lower frequency (From equation 2.1) than the lighter one and would be more stiffer. Theoretically, form the graph it is concluded that toolox 44 would be stiffer and have higher young's modulus than H13 as it is much heavier. This theory is proven by EMA done on the cutting tool when it is attached to the CNC machine and compliance graph is being plotted (ref. figure 4.2).

The modal data obtain through EMAs when the tool is attached to machine is being used to make the SLD for the machining test. Normal steel cutting force coefficient is chosen to plot the SLD, as it is much closer to toolox-33 force coefficient. More importantly, the aim is to see the trend and have vague idea of how the cutting tool will be perform during the machining test. In SLD, Toolox 44 shows a significant increase in higher resistance to chatter than H13 at different RPMs.

The machining tests is beginning designed by determining the parameter range such as depth of cut and cutting speed by taking into account the cutting tool diameter and insert specification. The RPM is chosen from the SLD keeping in mind the recommended range. The throughput (sound from the microphone) plotted at different RPM and depth of cut shows (figure 4.5) that Toolox is being stable at higher depth cut at each RPM it has run from H13. The waterfall graph (figure 4.6) is plotted at these points' shows that the system is going into chatter and forced vibrations are well around the eigen frequencies of the tools hence proving the EMA test done attached to the machine structure. The surface roughness test is being conduct on machined surface the points where toolox 44 is stable and H13 is not. It has been found by comparison that the Ra is less for all those points. Thus giving a physical evidence that the surface quality is remain enacted even at higher Ap for toolox 44 (figure 4.7).

Even if the cutting tool material is compared by manufacturing point of view (Ref. chapter 4 Cutting tool material review) , toolox 44 does not have to go through any hardness or stress

reliving process after heavy machining thereby it is ready to use just after that. As for H13 steel which has to go through hardness and stress reliving process which in-turn changes the dimension of the cutting that forces to add one more final machining process at the end.

From the EMAs, machining tests, and surface roughness measurement, and Cutting tool material review one can easily draw a conclusion that cutting tool made from toolox 44 has high material removal capacity and more resistance towards vibration than H13 steel without losing the surface quality at the recommended rpm. Moreover, it requires less time to manufacture and is more cost efficient while producing than the conventional steel.

6. Future work

The thesis has only scratched surface with comparing between two cutting tool of similar configuration. Toolox 44 steel has shown a huge potential usage in the tooling industry. There is huge scope of further work on the material like to get a wider comparison between the cutting tools, toolox 44 can be tested in different variation and different working condition such as variation in number of teethes, tool overhang diameter, sizes, distance between the teethes, in condition with or without coolant and the life-cycle of the inserts. The other possibility of research work can go into coating the tool holder by different damping coating. Even the cost comparison can be done both from manufacturing it as cutting tool and its usage in the production. A lot of research is being happening in KTH on cutting tool made up of conventional steel [1, 4, 12]. As this thesis showed that Toolox 44 is performing better than the convention steel, now they can focus on it.

7. Reference

1. Le Lan, J.-V., A. Marty, and J.-F. Debongnie, *A stability diagram computation method for milling adapted to automotive industry*, in *Second CIRP International Conference on High performance cutting*. Jun-2006: Vancouver.
2. Quintana, G. and J. Ciurana, *Chatter in machining processes: A review.* International Journal of Machine Tools and Manufacture, 2011. **51**(5): p. 363-376.
3. Ewins, D.J., *Modal testing: theory and practice*. 1984: Research Studies Press.
4. Ahid D. Nashif, D.I.J., and John P. Henderson, *Vibration Damping*. Vibration Damping. 1985: John Wiley & Sons Inc
5. Tobias, S.A., *Machine tool vibration research.* International Journal of Machine Tool Design and Research, 1961. **1**(1–2): p. 1-14.
6. Gurney, J.P. and S.A. Tobias, *A graphical method for the determination of the dynamic stability of machine tools.* International Journal of Machine Tool Design and Research, 1961. **1**(1–2): p. 148-156.
7. Österlind, T., *An Analysis of Machining System Capability and Its Link with Machined Component Quality*, in *KTH, School of Industrial Engineering and Management (ITM), Production Engineering, Machine and Process Technology.* 2013, KTH Royal Institute of Technology: Stockholm. p. 54.
8. Sweeney, G. and S.A. Tobias, *Survey of basic machine tool chatter research.* International Journal of Machine Tool Design and Research, 1969. **9**(3): p. 217-238.
9. Das, M.K. and S.A. Tobias, *The relation between the static and the dynamic cutting of metals.* International Journal of Machine Tool Design and Research, 1967. **7**(2): p. 63-89.
10. *Toolox 33/44 Brochures*. Toolox 33/44 Brochures]. Available from: http://www.ssab.com/Global/Toolox/Brochures/en/020_Toolox_a_better_concept_UK.pdf.
11. *Bohler-Uddeholm Tool steel Data sheet*, B.-U. CORPORATION, Editor. 07.2013.
12. Daghini, L., *Improving Machining System Performance through designed-in Damping : Modelling, Analysis and Design Solutions*. 2012, KTH Royal Institute of Technology: Stockholm.

Appendix I:

SSAB Toolox 33 (Material of the Workpiece)					
Chemical composition:- C-0.22-0.24%; Si-0.6-1.1% ; Mn-0.8% ; P- max 0.010%;S- max 0.003%; Cr-1.0-1.2%; Mo- 0.30%; V-0.10-0.11%; Ni- max 1% ; CEIIW- 0.62-0.71; CET- 0.40-0.44					
Physical Data:					
Temperature	+20°c		+200°c		+400°c
Heat conductivity [W/m K]	35		35		30
Thermal expansion coefficient, [10^{-6}/K]	13,1		13,1		
Mechanical Data:					
Temperature	+20°c	+200°c	+300°c	+400°c	+500°c
Tensile strength, R_m [MPa]	980	900			
Yield strength, $R_{p0,2}$[MPa]	850	800			
Elongation, A_s [%]	16	12			
Compressive yield strength, $R_{c0,2}$ [MPa]	800	750	700	590	560
Impact toughness [J]	100	170	180	180	
Hardness [HBW]	300				
Hardness [HRC]	29				

SSAB Toolox 44 (Material of the Cutting tool)					
Chemical composition:- C-0.32%; Si-0.6-1.1% ; Mn-0.8% ; P- max 0.010%;S- max 0.003%; Cr-1.35%; Mo- 0.80%; V-0.14%; Ni- max 1% ; CEIIW- 0.92-0.96; CET- 0.55-0.57					
Physical Data:					
Temperature	+20°c		+200°c		+400°c
Heat conductivity [W/m K]	34		32		31
Thermal expansion coefficient, [10^{-6}/K]	13,5		13,5		13,5
Mechanical Data:					
Temperature	+20°c	+200°c	+300°c	+400°c	+500°c
Tensile strength, R_m [MPa]	1450	1380			
Yield strength, $R_{p0,2}$[MPa]	1300	1200			
Elongation, A_s [%]	13	10			
Compressive yield strength, $R_{c0,2}$ [MPa]	1250	1120	1120	1060	930-910
Impact toughness [J]	30	60	80	80	
Hardness [HBW]	450				
Hardness [HRC]	45				

Appendix II:

BOHLER-UDDEHOLM H13 Tool Steel			
Chemical composition:- C-0,39% ;Si-1,0% ;Mn- 0,4%; Cr- 5,3%; Mo- 1,3%; V- 0,9%			
Standard Specification:- AISI H13; W.-Nr.1,2344 ; EN X40CrMoV5-1			
Physical Data:			
Temperature	+20°c	+400°c	+1110°c
Density (kg/m^3)	7800	7700	7600
Modulus of Elasticity (N/mm^2or Pa)	210000	180000	140000
Coefficient of thermal expansion (per °c from 20°c)		12,6 x 10^{-6}	13,2 x 10^{-6}
Thermal conductivity (W/m°C)	25	29	30
Mechanical Properties:			
Hardness	52HRC	45HRC	
Tensile strength (UTS Rm) (N/mm^2)	1820	1420	
Yield strength(YS $Rp_{0,2}$) (N/mm^2)	1520	1280	

Appendix III:

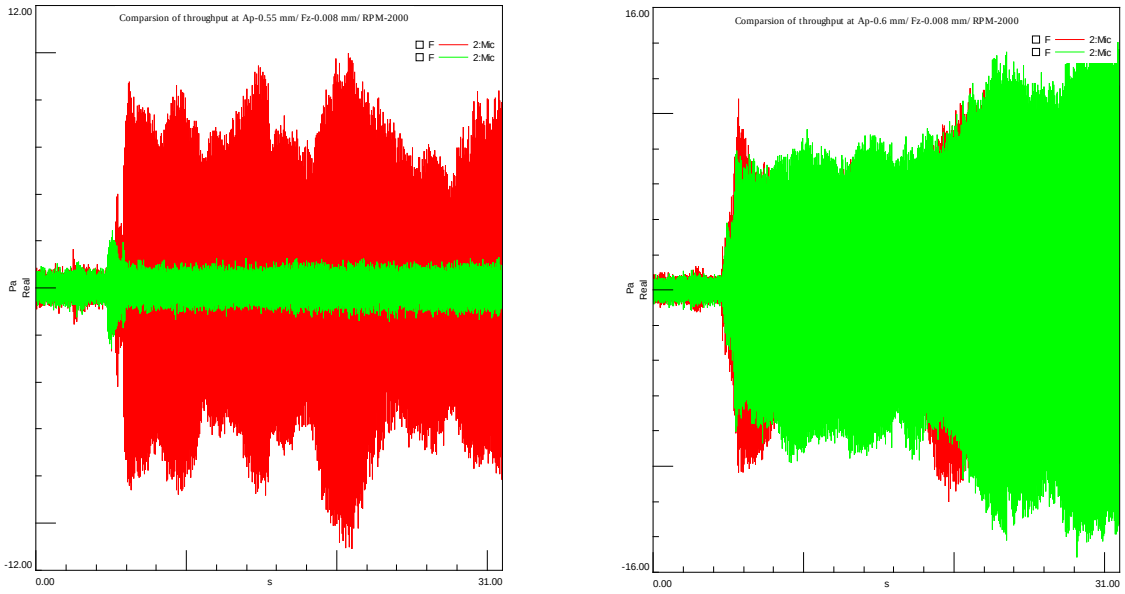

Figure 1: Comparison of Throughput at 2000 rpm (left) Ap-0.55 mm (right) Ap-0.60 mm [Toolox- Green; H13-Red]

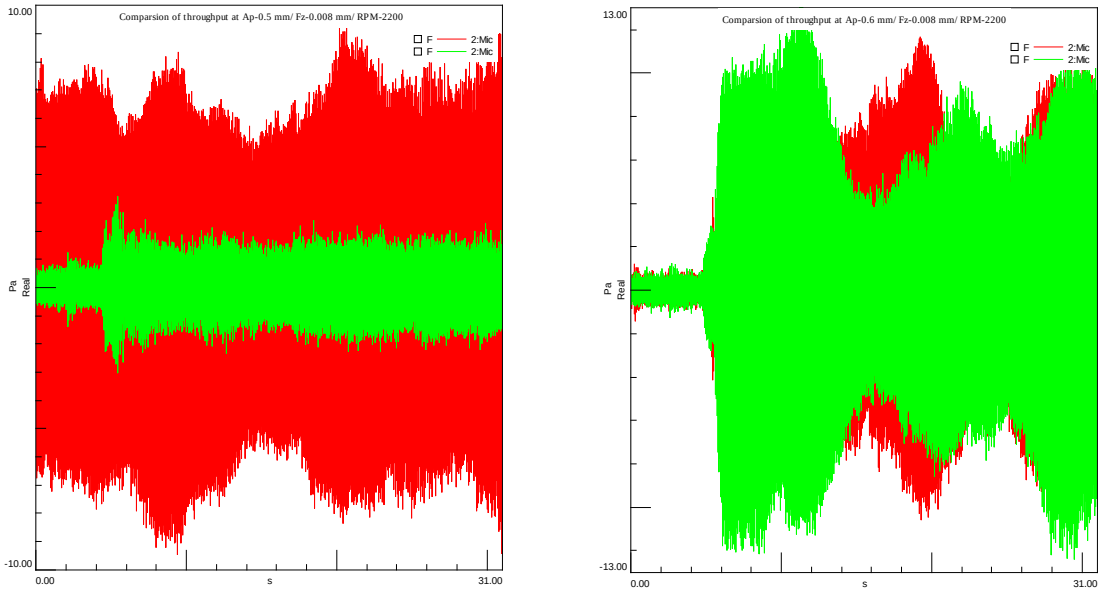

Figure 2: Comparison of Throughput at 2200 rpm (left) Ap-0.50 mm (right) Ap-0.60 mm [Toolox- Green; H13-Red]

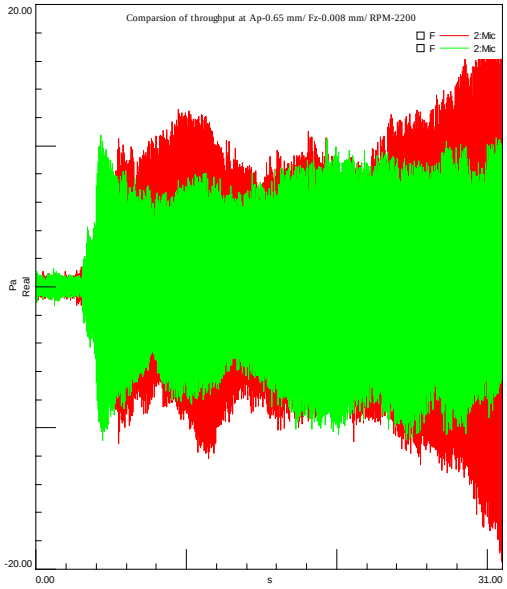

Figure 3: Comparison of Throughput at 2300 rpm (left) Ap-0.65 mm [Toolox- Green; H13-Red]

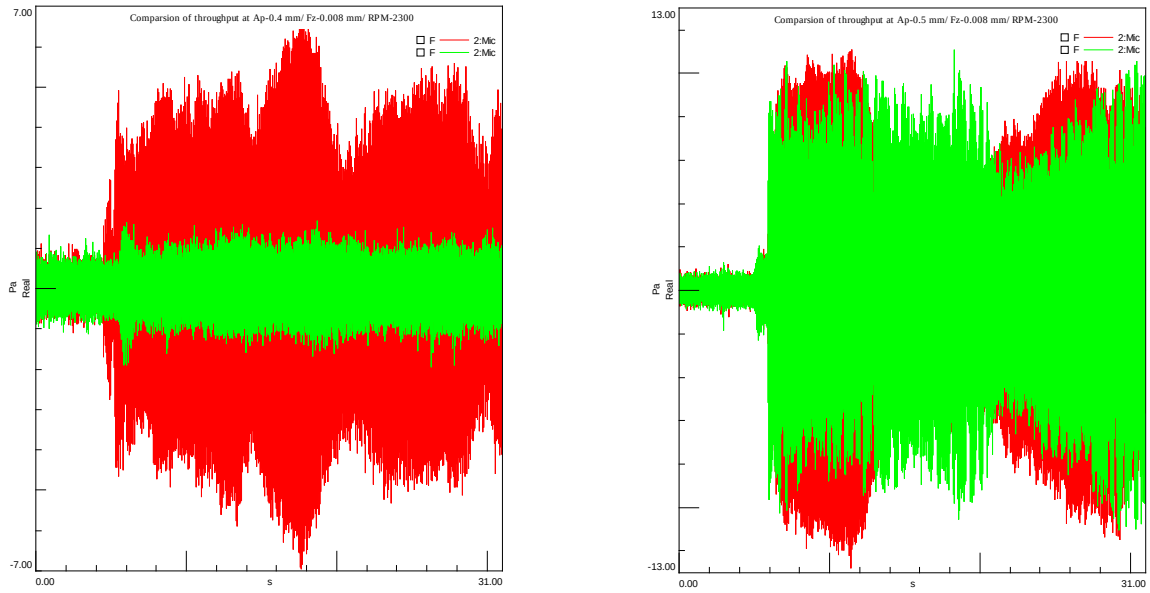

Figure 4: Comparison of Throughput at 2300 rpm (left) Ap-0.40 mm (right) Ap-0.50 mm [Toolox- Green; H13-Red]

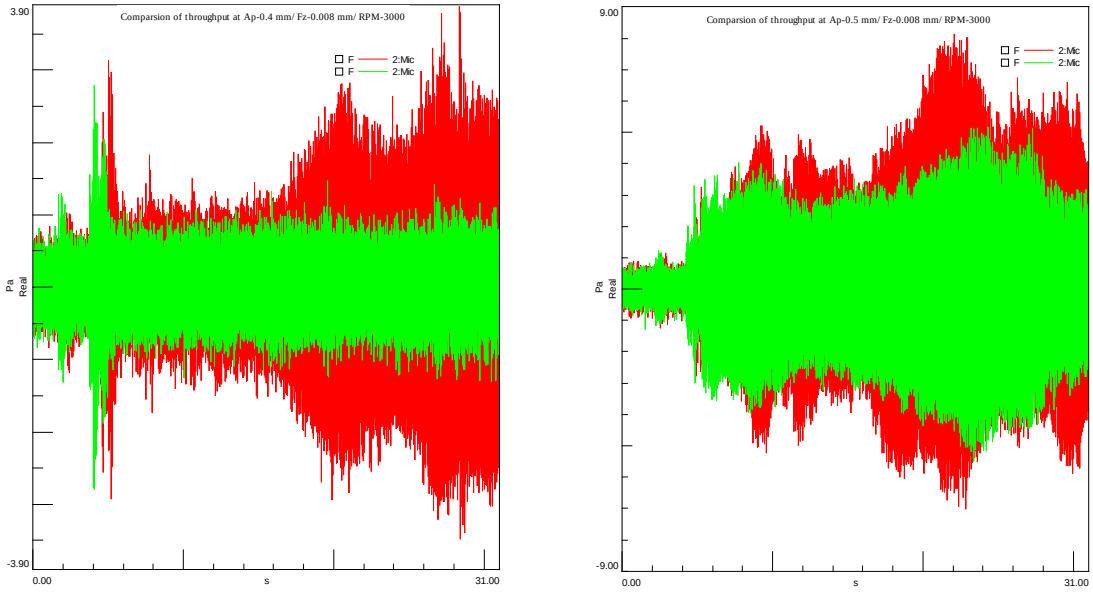

Figure 5: Comparison of Throughput at 3000 rpm (left) Ap-0.40 mm (right) Ap-0.50 mm [Toolox- Green; H13-Red]

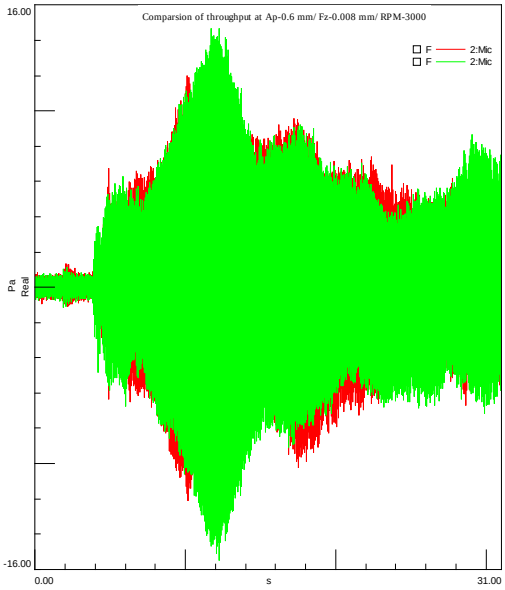

Figure 6: Comparison of Throughput at 3000 rpm (left) Ap-0.60 mm [Toolox- Green; H13-Red]

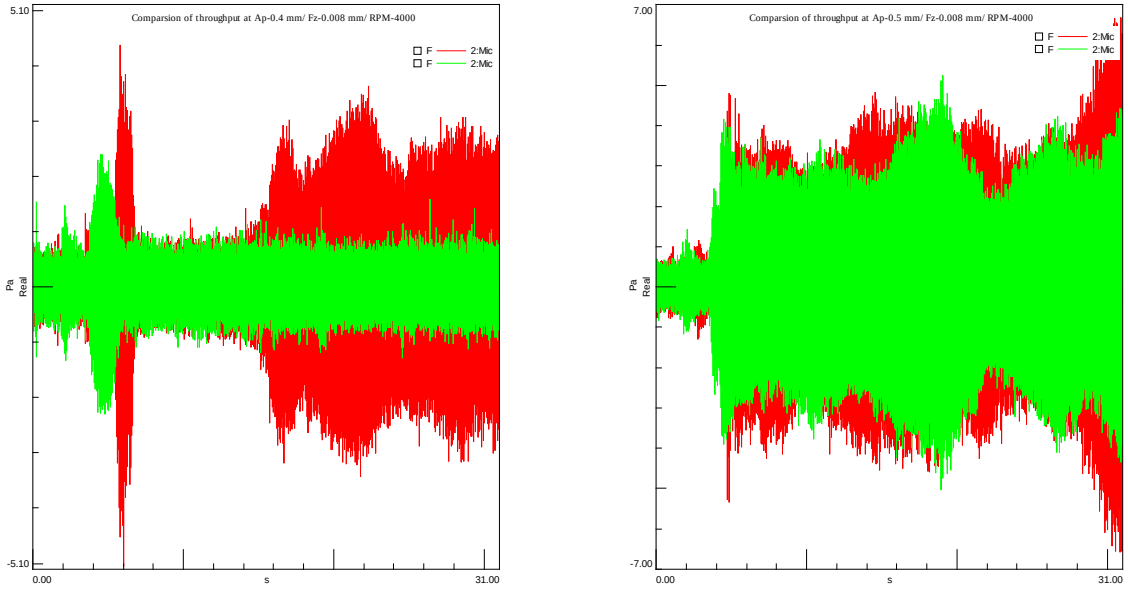

Figure 7: Comparison of Throughput at 4000 rpm (left) Ap-0.40 mm (right) Ap-0.50 mm [Toolox- Green; H13-Red]

Appendix IV:

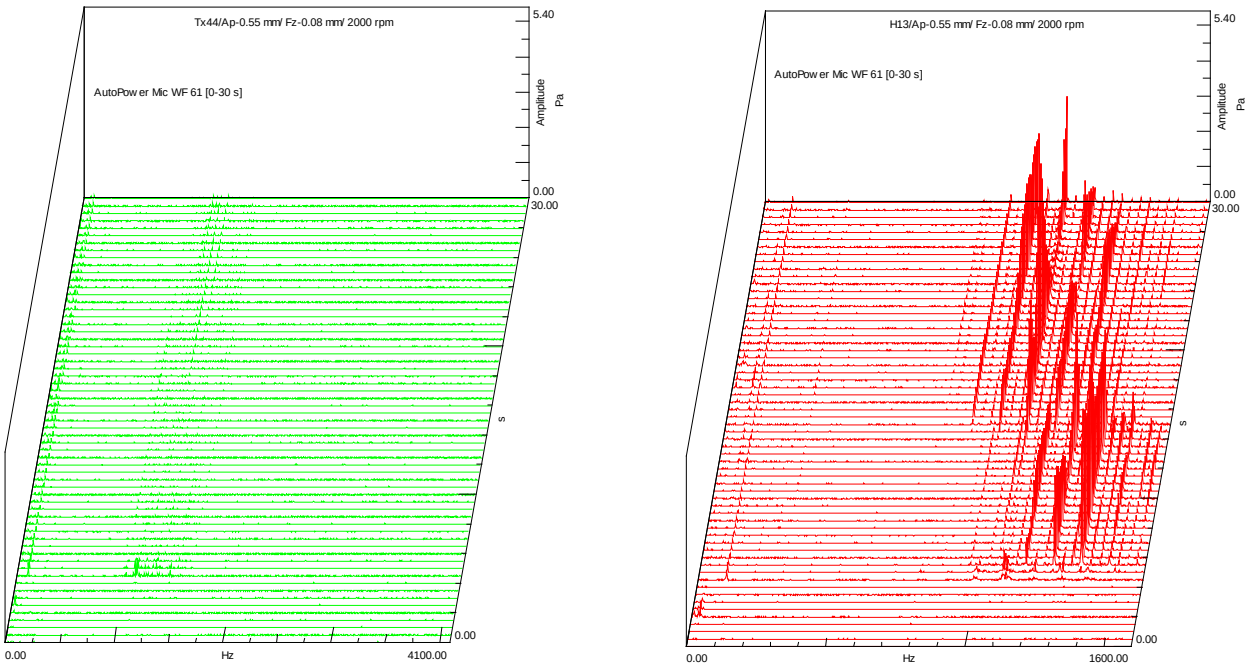

Figure 8: Comparison of waterfall plot at 2000-rpm Ap-0.55 mm [Toolox- Green; H13-Red]

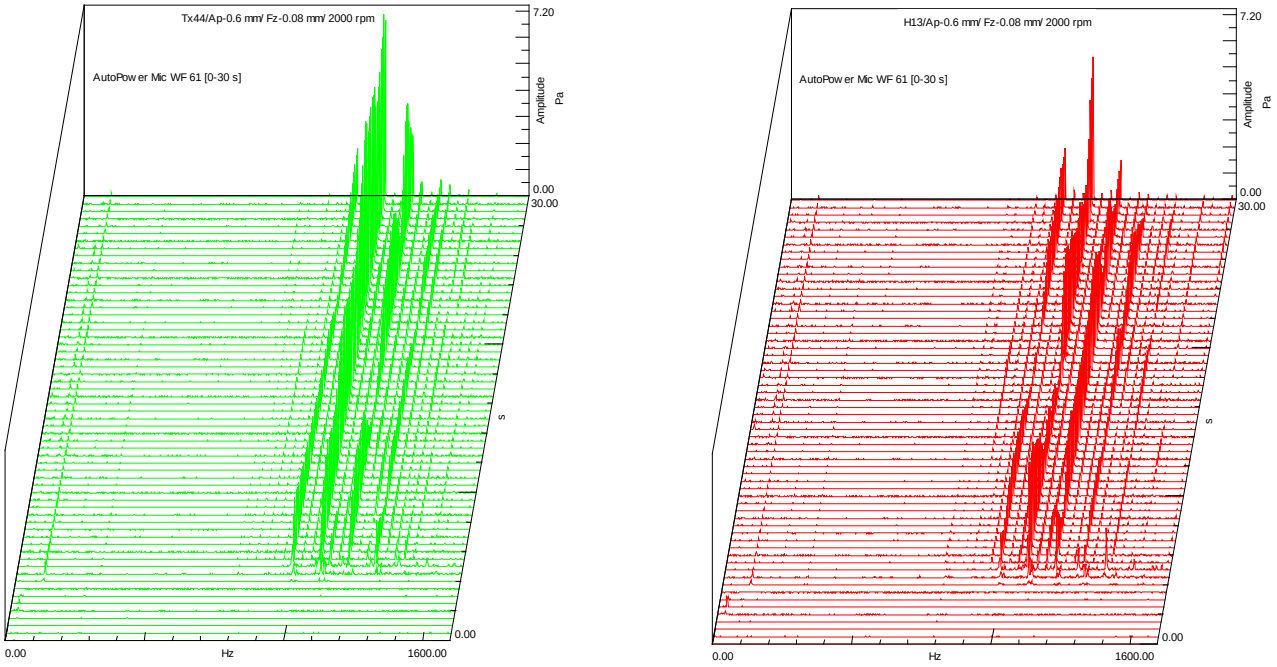

Figure 9: Comparison of waterfall plot at 2000-rpm Ap-0.6 mm [Toolox- Green; H13-Red]

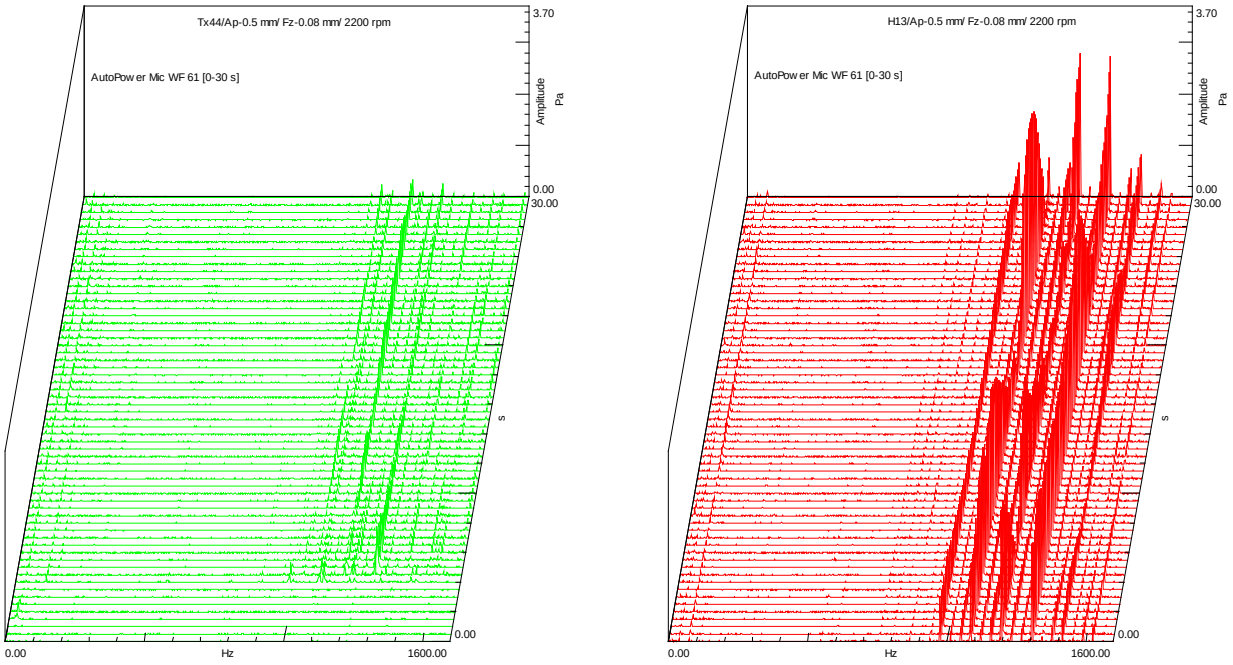

Figure 10: Comparison of waterfall plot at 2200-rpm Ap-0.5 mm [Toolox- Green; H13-Red]

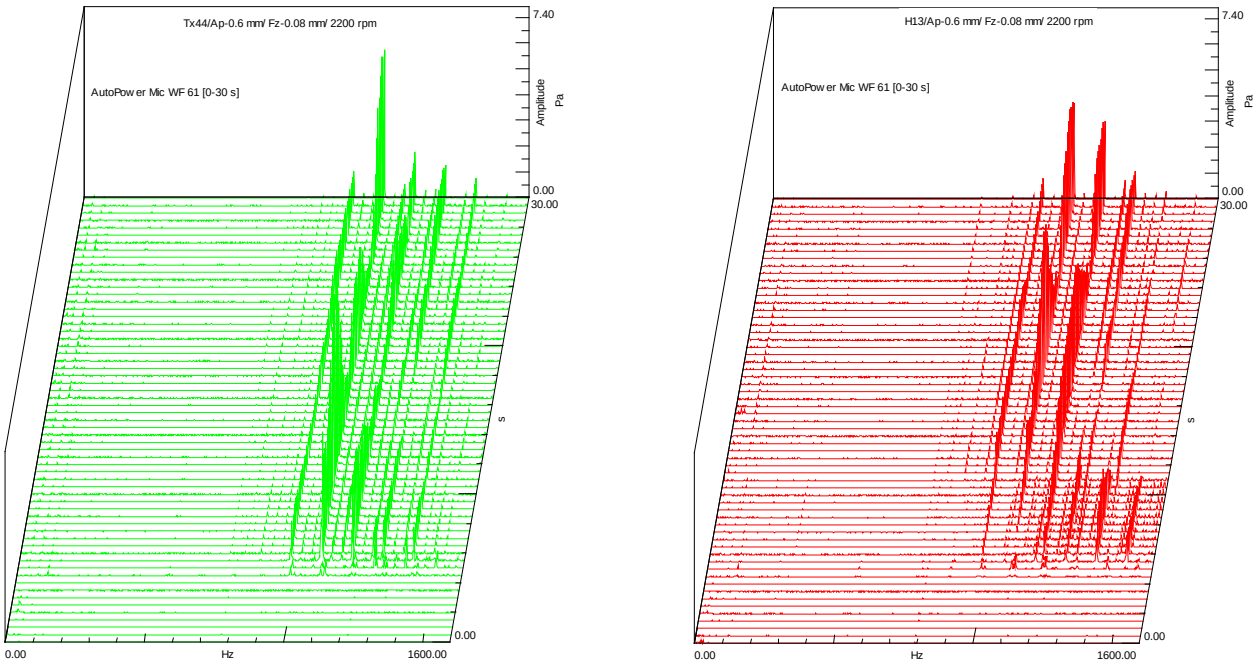

Figure 11: Comparison of waterfall plot at 2200-rpm Ap-0.5 mm [Toolox- Green; H13-Red]

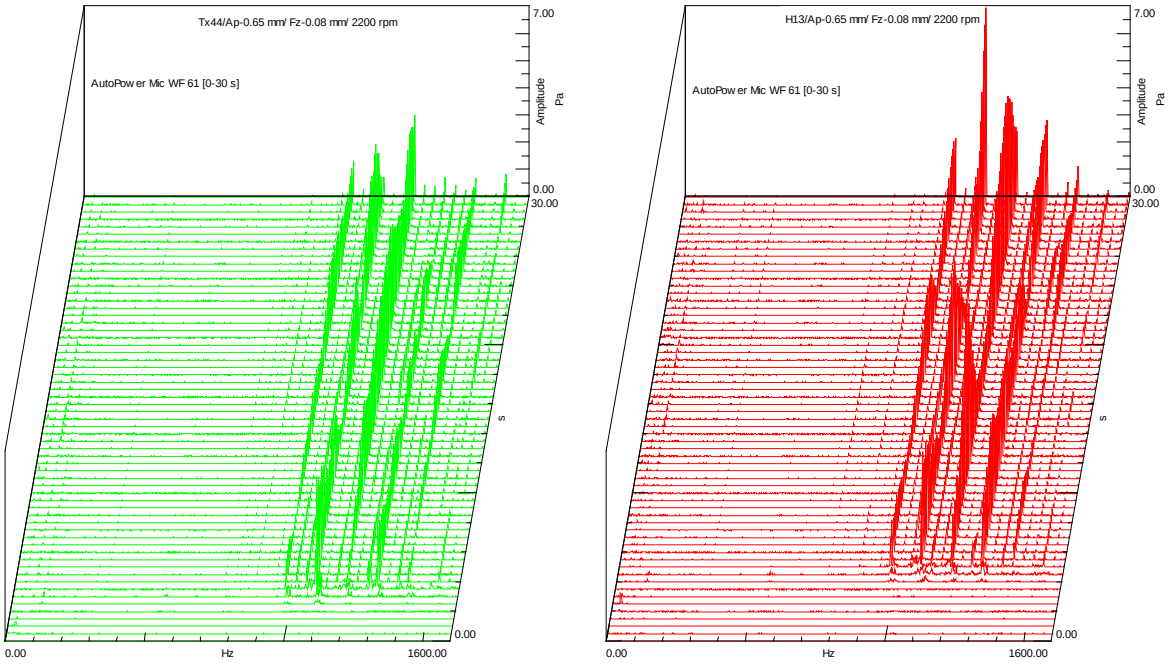

Figure 12: Comparison of waterfall plot at 2200-rpm Ap-0.65 mm [Toolox- Green; H13-Red]

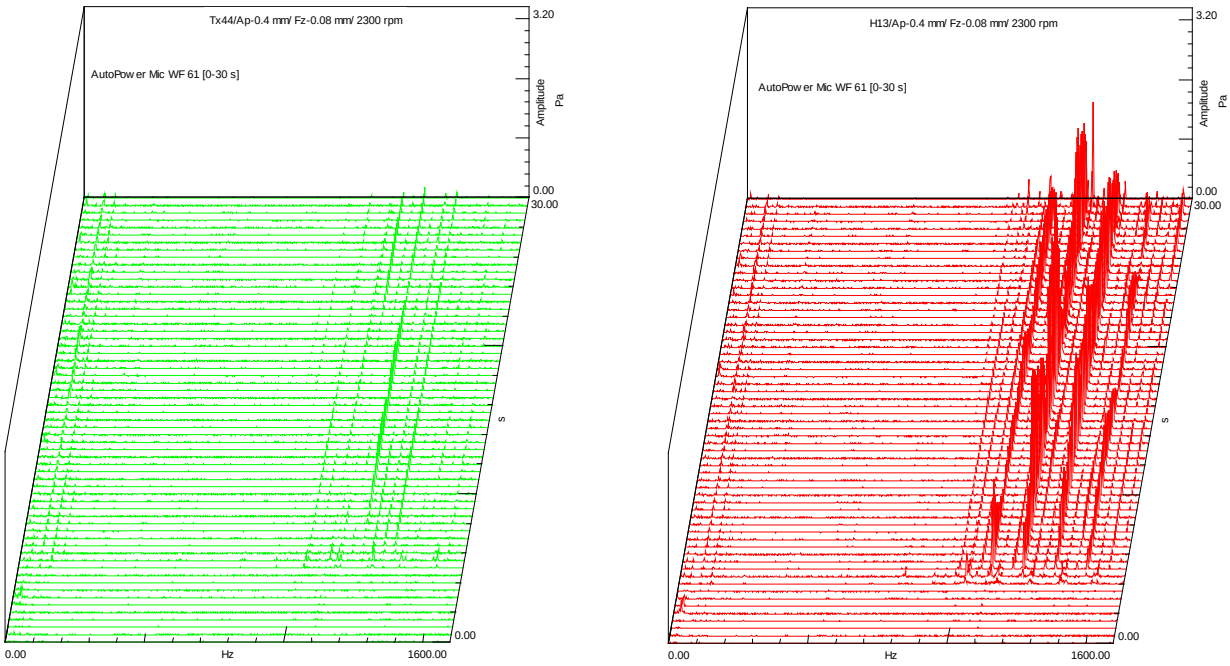

Figure 13: Comparison of waterfall plot at 2300-rpm Ap-0.4 mm [Toolox- Green; H13-Red]

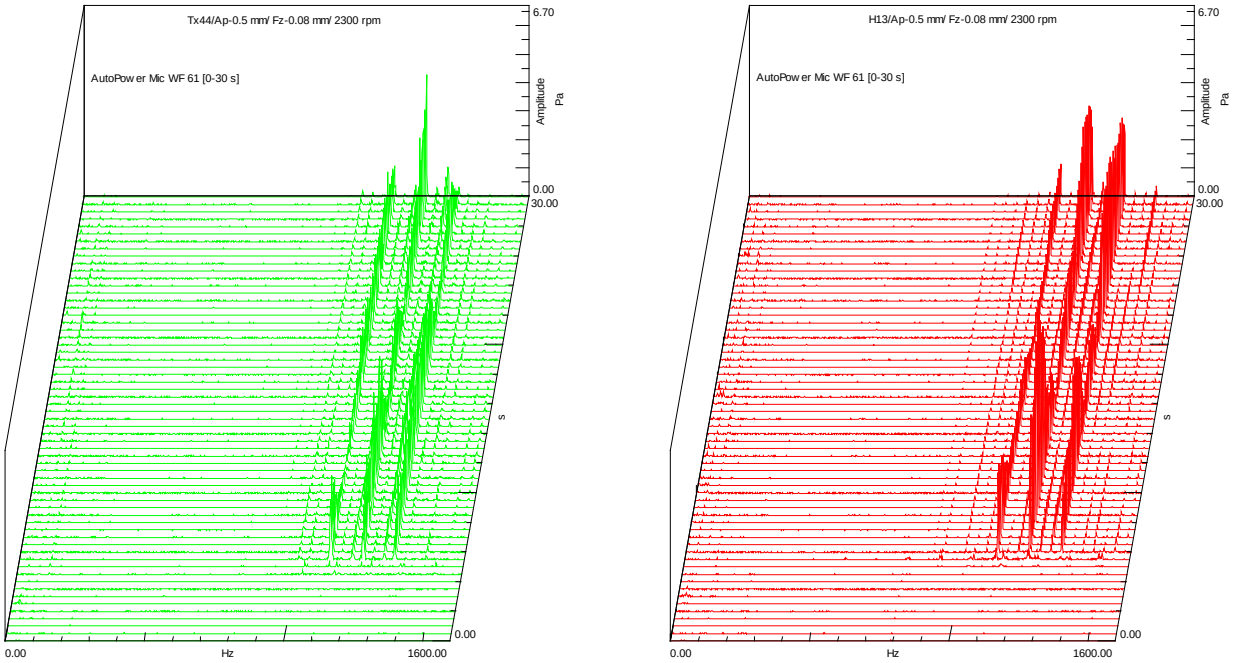

Figure 14: Comparison of waterfall plot at 2300-rpm Ap-0.5 mm [Toolox- Green; H13-Red]

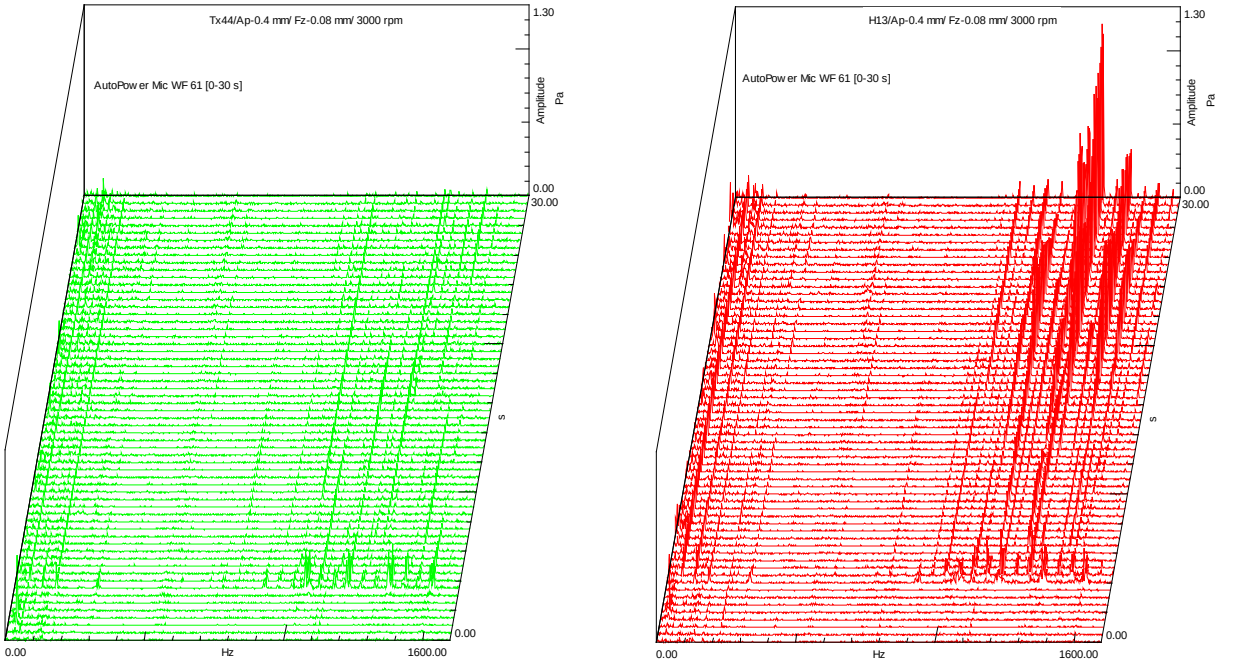

Figure 15: Comparison of waterfall plot at 3000-rpm Ap-0.4 mm [Toolox- Green; H13-Red]

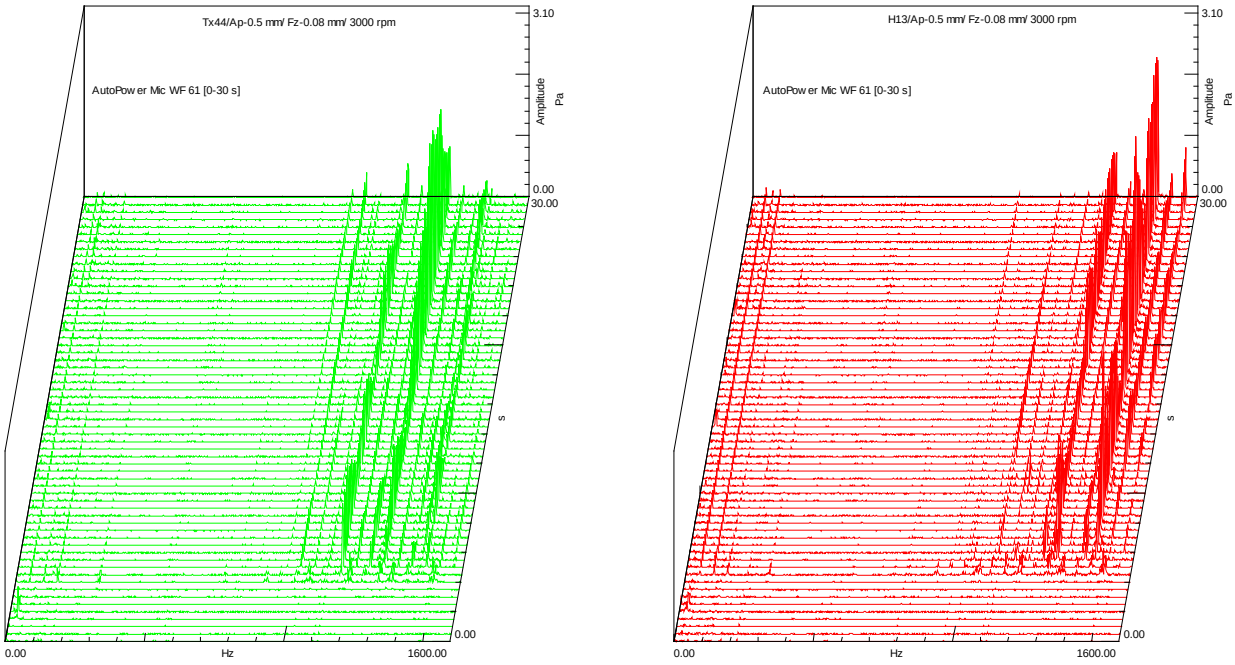

Figure 16: Comparison of waterfall plot at 3000-rpm Ap-0.5 mm [Toolox- Green; H13-Red]

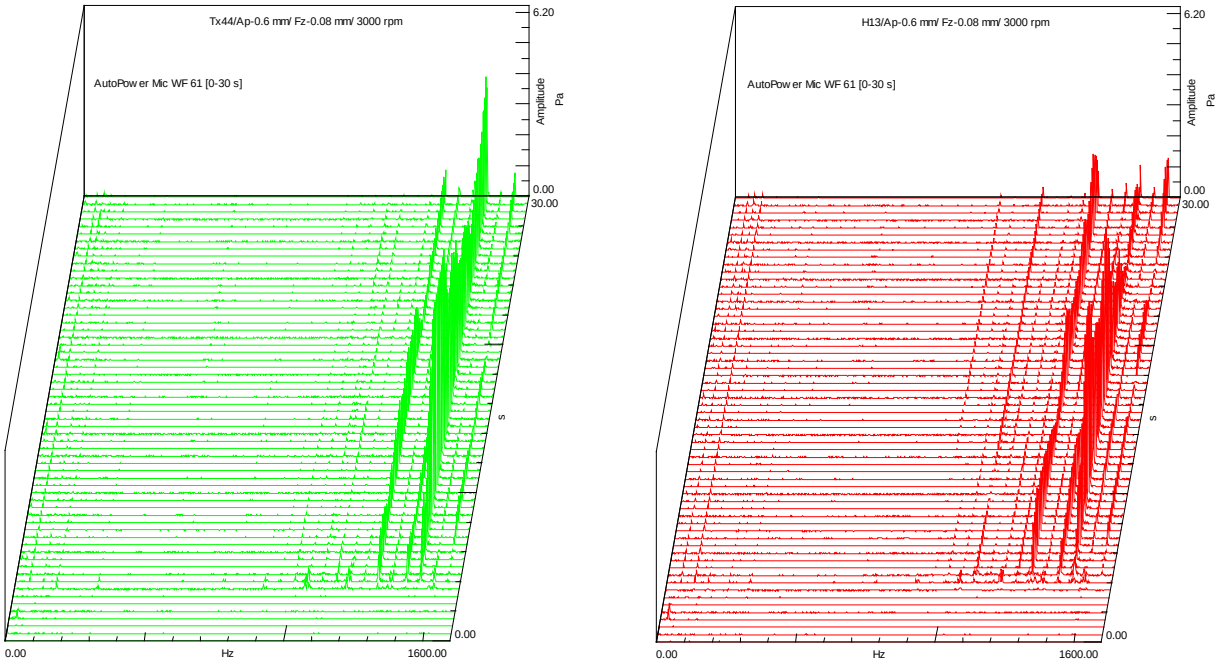

Figure 17: Comparison of waterfall plot at 3000-rpm Ap-0.6 mm [Toolox- Green; H13-Red]

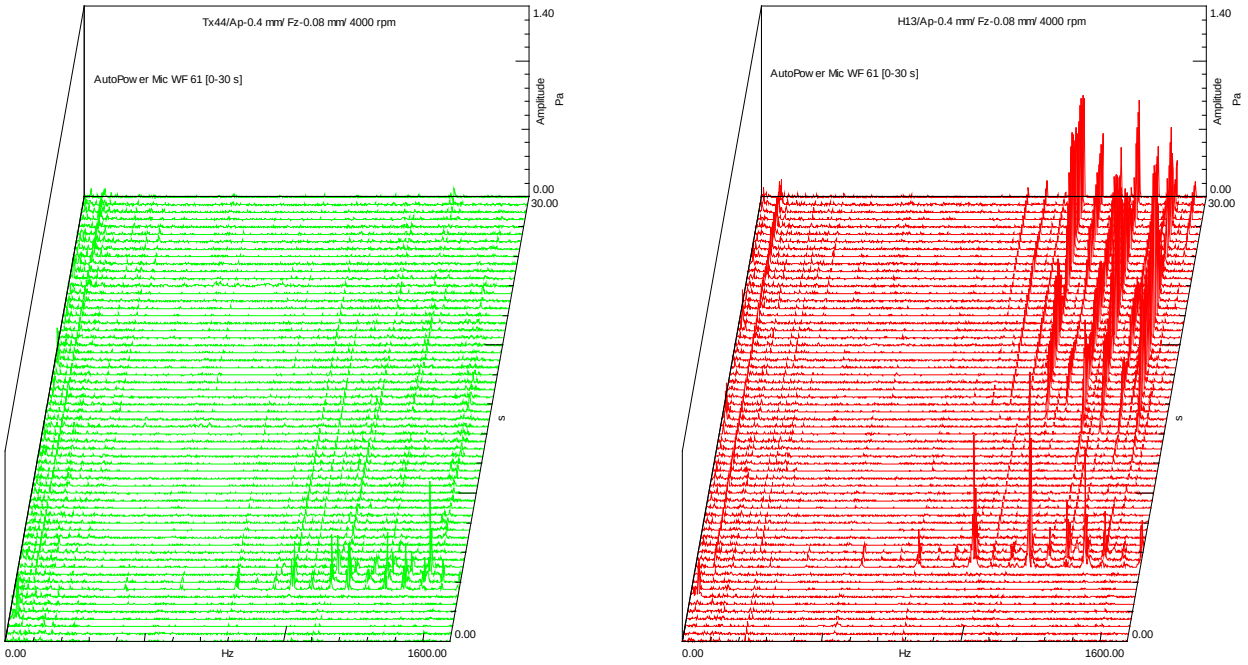

Figure 18: Comparison of waterfall plot at 4000-rpm Ap-0.4 mm [Toolox- Green; H13-Red]

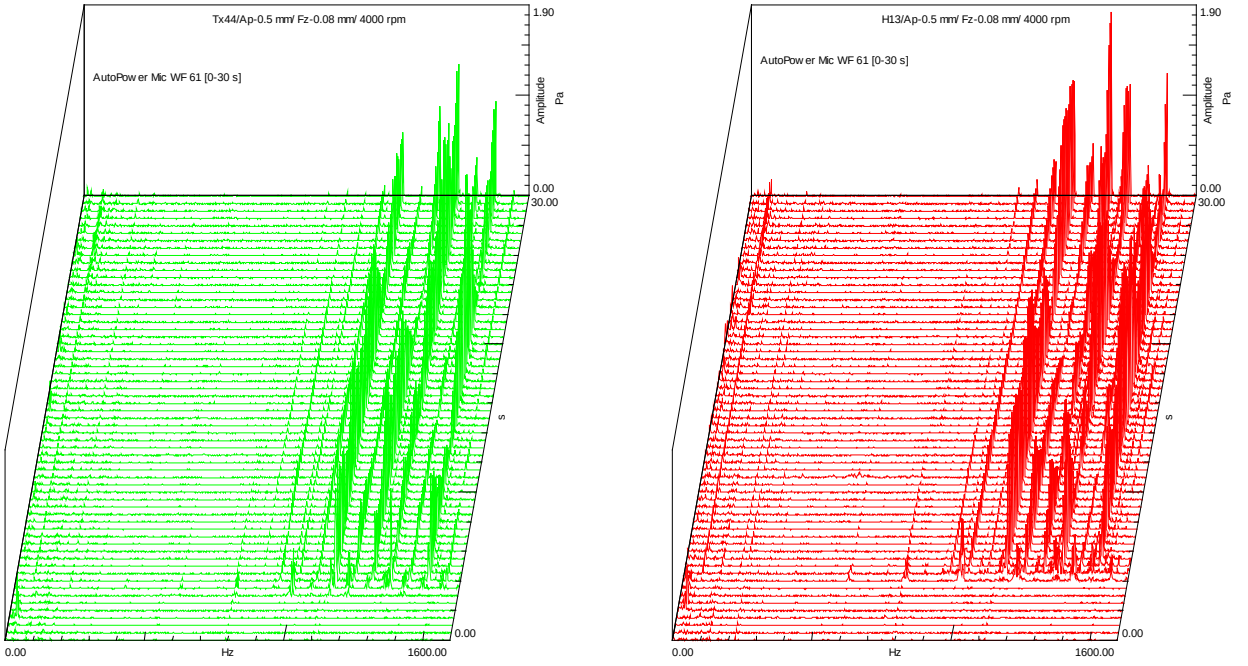

Figure 19: Comparison of waterfall plot at 4000-rpm Ap-0.5 mm [Toolox- Green; H13-Red]

Appendix V:

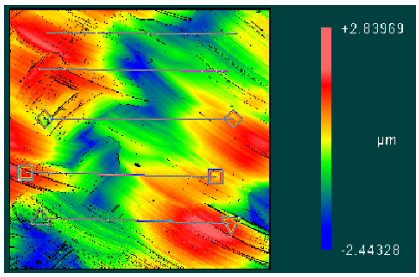

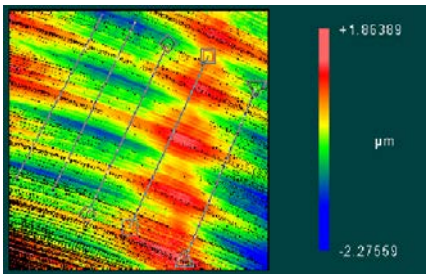

PV	5.283 µm	PV	4.139 µm
RMS	0.887 µm	RMS	0.572 µm
R_a	0.740 µm	R_a	0.464 µm

Figure 20: Comparison of Surface roughness (Left) H13 Ap-0.55mm Rpm-2000 (Right) Toolox44 Ap-0.55mm Rpm-2000

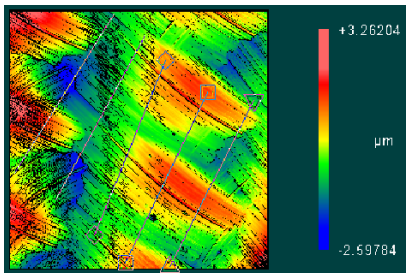

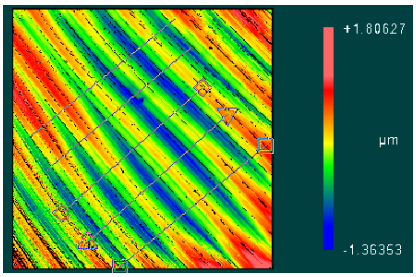

PV	5.860 µm	PV	3.170 µm
RMS	0.867 µm	RMS	0.457 µm
R_a	0.709 µm	R_a	0.367 µm

Figure 21: Comparison of Surface roughness (Left) H13 Ap-0.5mm Rpm-2200 (Right) Toolox 44 Ap-0.50mm Rpm-2200

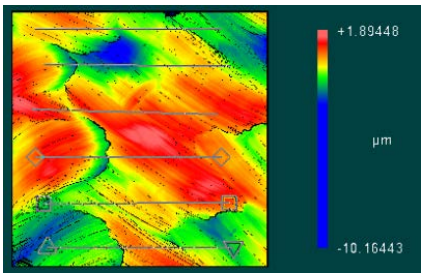

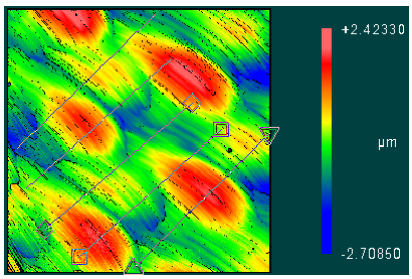

PV	12.059 µm	PV	5.132 µm
RMS	0.830 µm	RMS	0.782 µm
R_a	0.681 µm	R_a	0.618 µm

Figure 22: Comparison of Surface roughness (Left) H13 Ap-0.60 mm Rpm-2200 (Right) Toolox 44 Ap-0.60 mm Rpm-2200

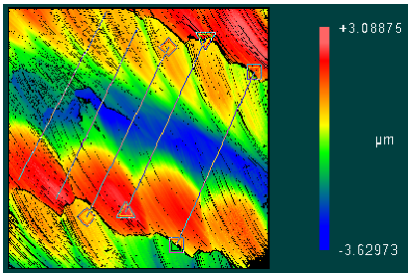

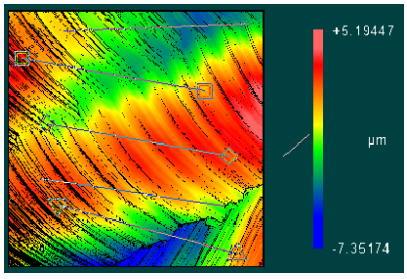

PV	6.718 µm	PV	12.546 µm
RMS	1.411 µm	RMS	2.141 µm
R_a	1.169 µm	R_a	0.784 µm

Figure 23: Comparison of Surface roughness (Left) H13 Ap-0.50 mm Rpm-2300 (Right) Toolox 44 Ap-0.50 mm Rpm-2300

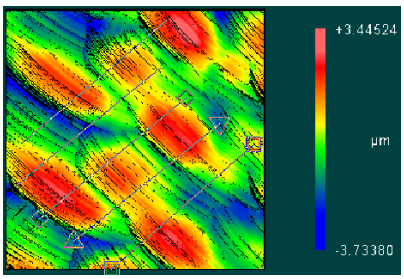

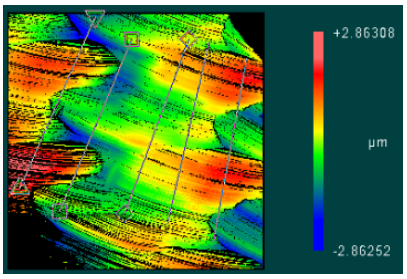

PV	7.179 µm	PV	5.726 µm
RMS	1.209 µm	RMS	0.858 µm
R_a	1.002 µm	R_a	0.689 µm

Figure 24: Comparison of Surface roughness (Left) H13 Ap-0.50 mm Rpm-3000 (Right) Toolox 44 Ap-0.50 mm Rpm-3000

Appendix VI:


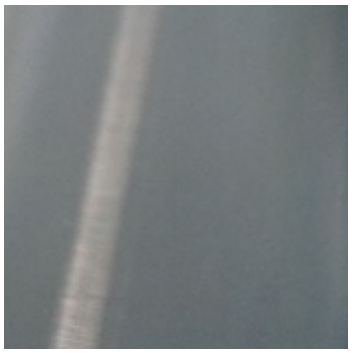

Figure 25: Picture comparing the (Left) H13 Ap-0.55mm Rpm-2000 (Right) Toolox 44 Ap-0.55mm Rpm-2000

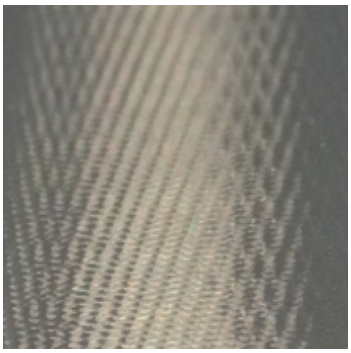
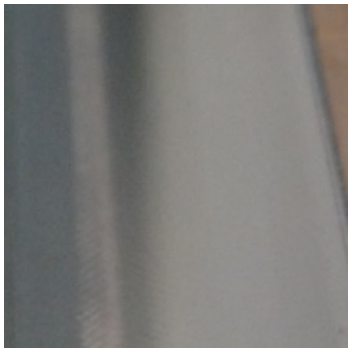

Figure 26: Picture comparing the (Left) H13 Ap-0.5mm Rpm-2200 (Right) Toolox 44 Ap-0.5mm Rpm-2200

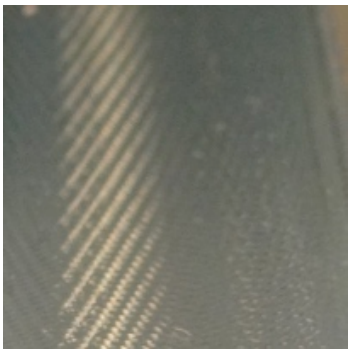
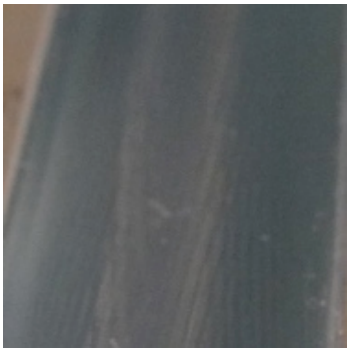

Figure 27: Picture comparing the (Left) H13 Ap-0.6mm Rpm-2200 (Right) Toolox 44 Ap-0.6mm Rpm-2200

Figure 28: Picture comparing the (Left) H13 Ap-0.5mm Rpm-2300 (Right) Toolox 44 Ap-0.5mm Rpm-2300

Figure 29: Picture comparing the (Left) H13 Ap-0.5mm Rpm-3000 (Right) Toolox 44 Ap-0.5mm Rpm-3000